Atmospheric chemical processing dictates aerosol aluminum solubility: insights from field measurement at two locations in Northern China

Tianyu Zhang,[1,5] Yizhu Chen,[1,5] Huanhuan Zhang,[2] Lei Liu,[3] Chengpeng Huang,[4] Zhengyang Fang,[1,a] Yifan Zhang,[1,5] Fu Wang,[4] Lan Luo,[4] Guohua Zhang,[1] Xinming Wang,[1] Mingjin Tang[1,6,*]

[1] State Key Laboratory of Advanced Environmental Technology and Guangdong Key Laboratory of Environmental Protection and Resources Utilization, Guangzhou Institute of Geochemistry, Chinese Academy of Sciences, Guangzhou, China

[2] Guangzhou Marine Geological Survey, China Geological Survey, Guangzhou, China

[3] Hangzhou International Innovation Institute, Beihang University, Hangzhou, China

[4] Longhua Center for Disease Control and Prevention of Shenzhen, Shenzhen, China

[5] College of Earth and Planetary Sciences, University of Chinese Academy of Sciences, Beijing, China

[6] Institute of Surface-Earth System Science, School of Earth System Science, Tianjin University, Tianjin, China

[a] Current address: Institute of Low Temperature Science, Hokkaido University, Sapporo, 060-0819, Japan

Correspondence: Mingjin Tang (mingjintang@126.com)

Abstract

Deposition of mineral dust aerosol into open oceans impacts marine biogeochemistry, and the deposition flux can be constrained using dissolved aluminum (Al) in surface seawater as a tracer. However, aerosol Al solubility, a critical parameter used in this method, remains highly uncertain. We investigated seasonal variations of aerosol Al solubility for supermicron and submicron particles at two locations (Xi'an and Qingdao) in Northern China. Aerosol Al solubility was very low at Xi'an, showed no apparent variation with seasons or relative humidity, and was not correlated with sulfate or nitrate; in contrast, Al solubility was much higher at Qingdao, exhibited distinct seasonal variability, and increased with relative humidity and the abundance of sulfate and nitrate. All these features observed for Al solubility at the two locations can be explained by the effects of atmospheric chemical processing. Mineral dust transported to Xi'an (an inland city in Northwest China) was still not obviously aged and thus chemical processing had little effect on aerosol Al solubility; after arriving at Qingdao (a coastal city in the Northwest Pacific), mineral dust was substantially aged by chemical processing, leading to significant enhancement in aerosol Al solubility. Our work further reveals that aerosol liquid water and acidity play vital roles in the dissolution of aerosol Al by atmospheric chemical processing. We suggest that chemical aging can lead to spatiotemporal variation of aerosol Al solubility, and this should be considered when using dissolved Al in surface seawater to constrain oceanic dust deposition.

1. Introduction

As an important type of tropospheric aerosols, mineral dust aerosol greatly impacts atmosphere chemistry, climate, and ecological systems (Jickells et al., 2005; Tang et al., 2016; Kok et al., 2023). After long-range transport, deposition of mineral dust into the oceans is a major external source of several nutrient and toxic elements for surface seawater (Moore et al., 2013; Westberry et al., 2023), impacting primary production and biogeochemical cycles in the oceans and having further feedback on the climate system (Mahowald, 2011; Jiang et al., 2024). The deposition flux of mineral dust aerosol into the oceans should be accurately estimated before we can assess its impacts on marine biogeochemistry in a reliable manner (Schulz et al., 2012; Anderson et al., 2016). Previous studies used several different methods to estimate dust deposition fluxes and found large discrepancies (Huneeus et al., 2011; Anderson et al., 2016).

Deposition of mineral dust aerosol is the dominant source of dissolved aluminum (Al) in the surface water of open oceans, and dissolved Al is generally considered to be chemically and biologically inactive in seawater. As a result, dissolved Al concentrations in surface seawater could be used to calculate dust deposition flux into the oceans (Measures and Brown, 1996; Measures and Vink, 2000), and the fractional solubility of aerosol Al (the fraction of aerosol Al that can be dissolved) is one of the key parameters used in this method. Previous studies which used this method to estimate dust depositions fluxes (Han et al., 2008; Measures et al., 2010; Grand et al., 2015; Benaltabet et al., 2022) usually assumed uniform Al solubility values in the range of 1.5-5%. However, field measurements found that aerosol Al solubility could vary by more than an order of magnitude (Baker et al., 2006; Buck et al., 2013), and thereby using a uniform aerosol Al solubility value could lead to large uncertainties in

estimated dust deposition fluxes (Han et al., 2008; Xu and Weber, 2021). In order to better constrain the oceanic dust deposition using dissolved Al in seawater as a tracer, we need to develop parameterizations for aerosol Al solubility, and this requires spatiotemporal variability of aerosol Al solubility to be understood and processes and mechanisms which drive such variations to be elucidated.

The initial Al solubility is generally low (typically <1.5%) for soil or mineral dust samples (Mulder et al., 1989; Duvall et al., 2008; Shi et al., 2011; Aghnatios et al., 2014; Li et al., 2022), and field studies found that aerosol Al solubility in the troposphere could be much higher and showed wide variability. For example, Al solubility ranged from 0.2-15.9% for total suspended particles (TSP) over the Pacific (Buck et al., 2013), and were in the range of 3-78% over the Atlantic (Buck et al., 2010; Chance et al., 2015). Some studies (Measures et al., 2010; Sakata et al., 2023) found good correlations between dissolved aerosol Al (or Al solubility) and acid species in aerosol particles, and thus suggested that chemical processes in the atmosphere could substantially enhance aerosol Al solubility; furthermore, Li et al. (2017) found that Al solubility was remarkably increased during cloud events when cloud processing enhanced the formation of secondary inorganic ions (mainly sulfate and nitrate) and thus increased the acidity of cloud droplets. However, Yang et al. (2023) found no correlations between Al solubility and the concentrations of aerosol acidic species, and concluded that the effect of acid processing on Al solubility was negligible. Aerosol Al solubility over the Atlantic appeared to be higher for air masses from Europe than those from the Saharan region (Baker et al., 2006; López-García et al., 2017), and some studies hypothesized that this could be potentially explained by the

87 influence of anthropogenic aerosol Al if it had higher solubility than mineral dust (Paris et al.,
88 2010; López-García et al., 2017).

89 It can be concluded that although aerosol Al solubility in the atmosphere was explored by
90 several previous studies, our understanding is still very limited. For example, it remains unclear
91 why aerosol Al solubility shows large spatial and temporal variation. Some work suggested
92 that atmospheric chemical aging could enhance aerosol Al solubility, but the mechanisms and
93 key environmental factors have not been elucidated. Furthermore, the effects of particle size
94 on aerosol Al solubility have not been well understood.

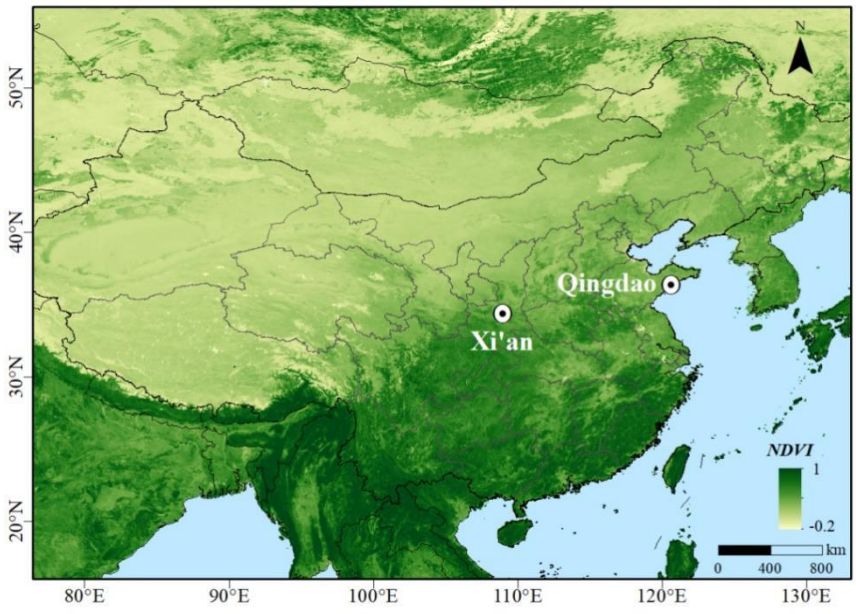

95

96 **Figure 1.** A map of East Asia and surrounding areas. The two locations (Xi'an and Qingdao)
97 where we collected aerosol particles are highlighted. NDVI: normalized difference vegetation
98 index provided by MODIS (Moderate Resolution Imaging Spectroradiometer).

99

100 In this work, we collected supermicron (>1 μm) and submicron (<1 μm) aerosol particles
101 at Xi'an and Qingdao, both located in Northern China, and investigated seasonal variations of

aerosol Al solubility at these two locations. Taklimakan and Gobi Deserts in Northwestern China are two important source regions of Asian dust (Prospero et al., 2002). As shown in Figure 1, Xi'an is an inland city in Northwestern China, located at the southern edge of the Loess Plateau which is also an active source of mineral dust (Cao et al., 2008; Jeong, 2020; Haugvaldstad et al., 2024), and the aging extent of mineral dust at Xi'an was found to be quite limited (Wang et al., 2014; Wu et al., 2017). As Asian dust is transported eastward, it passes over the North China Plain where anthropogenic emission is very high, and may become much more aged when arriving at Qingdao, a coastal city of the Northwest Pacific (Li et al., 2014; Pan et al., 2017). By comparing aerosol Al solubility at Xi'an and Qingdao, our work can provide valuable insights into how and to which extent aging processes during long-range transport can change aerosol Al solubility. Dust aerosol concentrations and meteorological conditions vary remarkably at different seasons in Northern China; as a result, examining its seasonal variations provides a good opportunity to understand the factors which regulate aerosol Al solubility.

2. Materials and methods

2.1 Sample collection

Samples were collected at two cities (Xi'an and Qingdao) in Northern China at four different seasons during 2021-2023 (Zhang et al., 2023; Chen et al., 2024), and further details can be found in the supplement (Text S1 and Table S1). In brief, supermicron (>1 μm) and submicron (<1 μm) particles were simultaneously collected using a two-stage aerosol sampler (TH-150C, Tianhong Co., China) which was operated at 100 L/min, and the sampling duration was typically 23.5 hours for each pair of aerosol samples. Whatman 41 cellulose filters were

used for aerosol collection in our work, and they were acid-washed before being used for aerosol sampling to reduce background levels (Zhang et al., 2022). A total of 126 and 106 pairs of aerosol samples were collected at Xi'an and Qingdao, respectively (Zhang et al., 2023; Chen et al., 2024). After collection, all the aerosol samples were stored at -20°C for further analysis.

In addition to aerosol particles, we also sampled atmospheric acidic and alkaline gases (mainly NH_3, HCl and HNO_3) at Qingdao, using a ChemComb 3500 Speciation Collection Cartridge (Thermo Fisher Scientific, USA) at a flow rate of 10 L/min (Walters and Hastings, 2018; Fang et al., 2025). Gas sampling was carried out concurrently with aerosol sampling. In brief, NH_3, HNO_3 and HCl were absorbed onto the inner walls of two tandem honeycomb diffusion tubes coated with proper adsorbents, and then converted into NH_4^+, NO_3^- and Cl^-. After the sampling was completed, 20 mL ultrapure water was used to rinse each tube immediately, and a PTFE membrane syringe filter (0.22 μm in pore size) was used to filter the solution. The solution was then frozen at -20°C for further analysis.

2.2 Sample analysis and aerosol acidity calculation

Sample pretreatment and analysis were detailed in our previous work (Zhang et al., 2022), and therefore are only briefly summarized here. The first half of a filter (and only one quarter of a filter for supermicron particles) was shredded and digested in a Teflon jar using a microwave digestion instrument. After digestion, the Teflon jar was filled with 1% HNO_3 (20 mL), and a PTFE membrane syringe filter (0.22 μm in pore size) was used to filter the solution; subsequently, the solution was analyzed by inductively coupled plasma-mass spectrometry (ICP-MS) to determine total concentrations of individual trace elements, including Al.

The other half of a filter was immersed in ultrapure water (20 mL) and stirred using an

orbital shaking for two hours; in the next step, the solution was filtered using a PTFE membrane syringe filter (0.22 μm in pore size) and divided into two parts. The first solution was acidified to contain 1% HNO_3 and subsequently analyzed by ICP-MS to determine the concentrations of dissolved trace elements; the second solution was analyzed by ion chromatography (IC) to quantify the concentration of water-soluble cations and anions.

The solutions obtained from honeycomb diffusion tubes (see Section 2.1 for more details) were also analyzed using IC to determine the concentrations of gaseous NH_3, HCl and HNO_3 in the atmosphere. ISORROPIA-II, a widely used aerosol thermodynamic model (Fountoukis and Nenes, 2007), was employed in this work to calculate the acidity of supermicron and submicron particles. It was operated in the forward mode, and aerosol particles were assumed to remain metastable. Input parameters included concentrations of water-soluble ions in aerosol particles and gaseous NH_3, HCl and HNO_3, temperature and relative humidity (RH). Our previous work found good agreement between measured and calculated NH_3 partitioning coefficients at Qingdao (Fang et al., 2025), and as a result the method we used could well estimate the acidity of supermicron and submicron particles.

3. Results

3.1 Seasonal variations of total and dissolved aerosol Al

3.1.1 Total aerosol Al

Figure 2 displays seasonal variations of total and dissolved aerosol Al at Xi'an and Qingdao. At Xi'an (Figure 2a), total Al in supermicron particles showed highest concentrations in spring and winter (1.54±0.89 and 1.91±0.93 $\mu g/m^3$) and lowest concentrations in summer (0.96±0.54 $\mu g/m^3$); a similar seasonal pattern was observed for submicron particles, with total

Al concentrations being highest in spring and winter (4.29±3.70 and 2.92±1.47 μg/m^3) and lowest in summer (0.95±0.44 μg/m^3). At Qingdao (Figure 2b), total Al concentrations in supermicron particles were highest in spring (1.04±1.12 μg/m^3) and lowest in summer and autumn (0.33±0.18 and 0.31±0.12 μg/m^3); similarly, for submicron particles, total Al concentrations were also highest in spring (1.88±2.51 μg/m^3) and lowest in summer and autumn (0.35±0.22 and 0.65±0.82 μg/m^3). For each season the median concentration of total aerosol Al was usually higher in submicron particles than supermicron particles at both locations (and there were some exceptions, as shown in Figures 1a and 1b). This is related to size dependence of mineralogy and elemental compositions of mineral dust aerosol, which is not well studied and deserves further investigation.

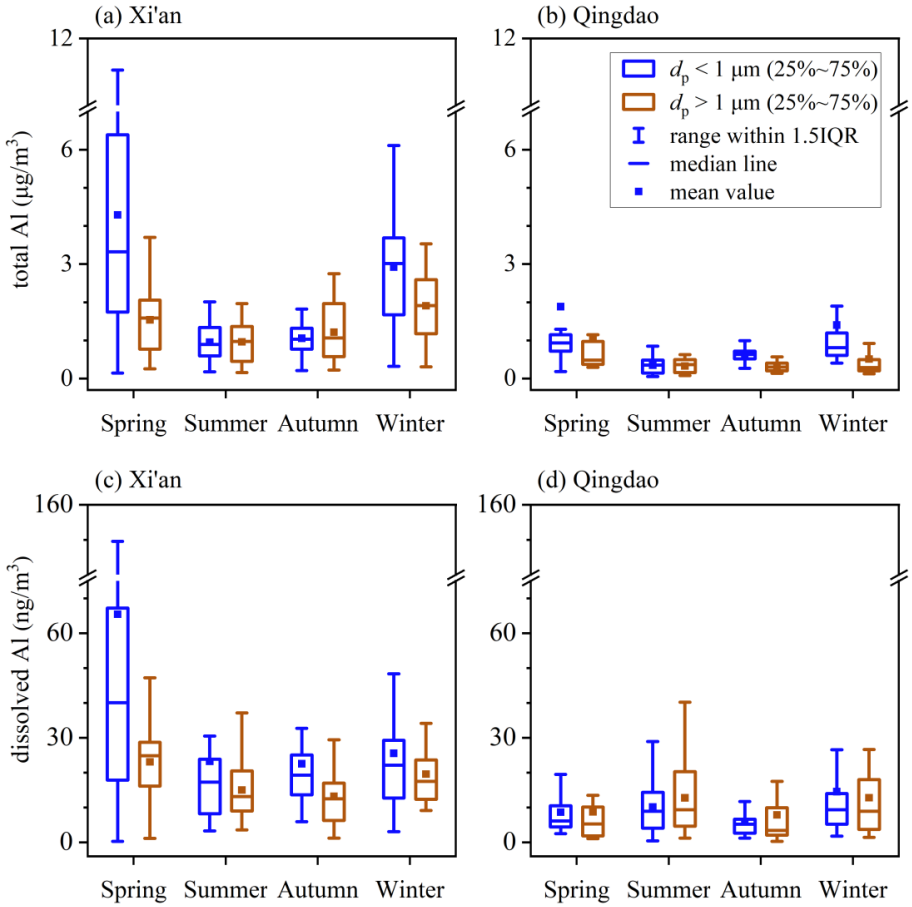

Figure 2. Seasonal variations of total and dissolved aerosol Al for submicron and supermicron

particles: (a) total Al at Xi'an; (b) total Al at Qingdao; (c) dissolved Al at Xi'an; (d) dissolved Al at Qingdao.

Overall, total aerosol Al concentrations showed similar seasonal variations at Xi'an and Qingdao, being highest in spring and lowest in summer. This was consistent with previous studies carried out in other locations in East Asia, such as Zhengzhou (Wang et al., 2019), Beijing (Zhang et al., 2013), Huaniao Island in the East China Sea (Guo et al., 2014), and Japan (Sakata et al., 2023). In East Asia, mineral dust aerosol was emitted into the atmosphere mainly in spring, leading to the increase in total aerosol Al concentrations. Lowest concentrations of total aerosol Al were observed in summer because precipitation in Northern China mainly occurred in summer, leading to enhanced wet deposition of aerosol particles (Cao and Cui, 2021). Furthermore, Qingdao was frequently affected by marine air masses in summer, and this is also one reason why total aerosol Al concentrations were lower in summer than other seasons. Total aerosol Al concentrations were higher in winter than summer and autumn at Xi'an, and one major reason is that meteorological conditions favored the accumulation of aerosol particles (including aerosol Al) during winter (Cao and Cui, 2021). Futhermore, besides spring, Asian dust also occurs in winter (Cai et al., 2020; Wang et al., 2020), and a previous study (Huang et al., 2014) suggested that the dust-related source, including local resuspended dust, contributed 56% to $PM_{2.5}$ during a severe haze event at Xi'an.

As summarized in the supplement (Table S2), total aerosol Al concentrations exhibited evident spatial variations in East Asia. As Asian dust was transported eastward to the North Pacific, a clear decrease in aerosol Al concentrations was observed. Mineral dust was the

dominant source for aerosol Al, and therefore concentrations of aerosol Al were found to be very high in desert regions. For example, total Al concentrations in TSP could reach 24 μg/m^3 over the Taklimakan Desert (Zhang et al., 2003). In our current study, annual average total Al concentrations at Xi'an, an inland city close to the desert, were reported to be 1.42±0.86 and 2.28±2.35 μg/m^3 for supermicron and submicron particles, much lower than that observed over the Taklimakan Desert. Further decrease in total Al concentrations was observed in coastal and oceanic regions. For example, our work found that the annual average total Al concentrations were 0.56±0.75 and 1.08±1.67 μg/m^3 for supermicron and submicron particles at Qingdao, lower than those at Xi'an; total Al concentrations in TSP ranged from 0.17 to 1.72 μg/m^3 in Hiroshima (Sakata et al., 2023), and further decreased to 1-56 ng/m^3 in Hawaii in the central Pacific (Measures et al., 2010).

3.1.2 Dissolved aerosol Al

At Xi'an (Figure 2c), for supermicron particles, dissolved aerosol Al concentrations were highest in spring (23.1±10.9 ng/m^3) and lowest in summer and autumn (15.0±8.7 and 13.2±8.6 ng/m^3); for submicron particles, dissolved Al concentrations were also highest in spring (65.4±79.2 ng/m^3) and lowest in summer and autumn (23.2±23.4 and 22.6±20.1 ng/m^3). Total (Figure 2a) and dissolved aerosol Al (Figure 2c) showed similar seasonal patterns at Xi'an, indicating that dissolved aerosol Al was mainly regulated by total aerosol Al.

As shown in Figure 2d, the average dissolved aerosol Al concentrations were 8.8±10.8, 12.8±11.1, 7.9±10.5 and 12.8±12.9 ng/m^3 for supermicron particles at Qingdao in spring, summer, autumn, and winter, respectively, and 8.7±5.8, 10.2±8.2, 6.0±4.8 and 14.5±15.2 ng/m^3 for submicron particles. Dissolved aerosol Al concentrations were highest in summer and

winter and lowest in autumn for both supermicron and submicron particles. In contrast to Xi'an, total and dissolved aerosol Al at Qingdao showed different seasonal patterns (Figures 2b and 2d); for example, total Al concentrations were lowest in summer at Qingdao when dissolved Al concentrations were highest. This indicates that dissolved aerosol Al at Qingdao was not only regulated by total aerosol Al but also affected by other factors such as atmospheric aging processes.

Compared to Xi'an, dissolved Al concentrations at Qingdao were lower across all the four seasons, mainly because total Al concentrations were much lower at Qingdao (Tables S3-S4 in the supplement). As shown in Figure 2, similar seasonal patterns were observed at two locations for total aerosol Al, but dissolved aerosol Al showed very different seasonality; this suggests that seasonal patterns of aerosol Al solubility were different at Xi'an and Qingdao, as presented in Section 3.2.

3.2 Fractional solubility of aerosol Al

3.2.1 Seasonal variations of Al solubility

Figure 3 displays aerosol Al solubility in different seasons at Xi'an and Qingdao. The median solubilities of aerosol Al were determined to be 1.38%, 1.59%, 1.04% and 1.01% for supermicron particles at Xi'an in spring, summer, autumn and winter, respectively, and 1.01%, 1.69%, 1.82% and 0.74% for submicron particles. Aerosol Al solubilities were generally low for the four seasons at Xi'an, showing no apparent variation with seasons (Figure 3a). In contrast, aerosol Al solubilities exhibited distinct seasonal variability at Qingdao (Figure 3b), and the median Al solubilities were highest in summer (3.56% and 2.33%) and lowest in spring (0.54% and 0.61%) for both supermicron and submicron particles.

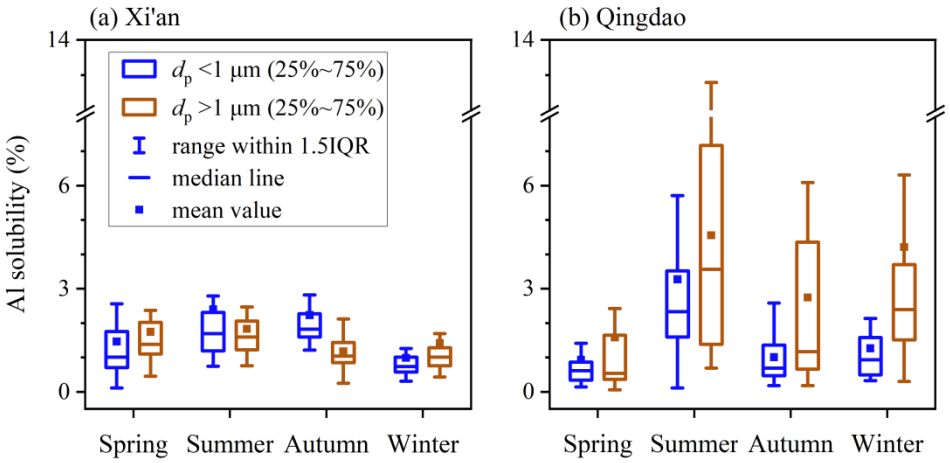

246

247 **Figure 3.** Seasonal variations of aerosol Al solubility for submicron and supermicron particles

248 at (a) Xi'an and (b) Qingdao.

249

250 In three seasons (summer, autumn and winter), aerosol Al solubility at Qingdao was

251 higher than that at Xi'an (Figure 3, Table S5). There are several important dust sources in

252 Northwest China, being far from (up to a few thousand km) or close to Xi'an. More importantly,

253 anthropogenic emission in Northwest China is much smaller than the North China Plain, and

254 thus the aging extent of mineral dust transported to Xi'an was rather limited (Wang et al., 2014;

255 Wu et al., 2017). On the contrary, Qingdao is much farther from deserts; consequently, after

256 long-distance transport over the North China Plain where anthropogenic emission is very large,

257 mineral dust aerosol which arrived at Qingdao was substantially aged (Trochkine et al., 2003;

258 Takahashi et al., 2011; Jeong, 2020), thereby leading to enhanced dissolution of aerosol Al and

259 thus the increase in Al solubility. Mineral dust from different desert regions and local

260 suspended dust cannot explain higher Al aerosol solubility observed at Qingdao, as previous

261 work showed that Al solubility was low for soil samples from different regions (Mulder et al.,

262 1989; Duvall et al., 2008; Shi et al., 2011; Aghnatios et al., 2014; Li et al., 2022).

On the other hand, no obvious difference in aerosol Al solubility was observed between Xi'an and Qingdao in spring, with median aerosol Al solubilities being <1.4% for supermicron and submicron particles (Figure 3). This agrees with a previous study (Hsu et al., 2010) which found that aerosol Al solubility was very low (average: ~0.7%) in spring even over the East China Sea. Furthermore, similar to what we observed in spring at Xi'an and Qingdao, Al solubility was found to be low (<1.5%) for surface soil particles (Mulder et al., 1989; Duvall et al., 2008; Shi et al., 2011; Aghnatios et al., 2014; Li et al., 2022). Overall, our work implies that in spring when Asian dust occurred most frequently, mineral dust particles arriving at Qingdao after long-distance transport did not show substantial increase in Al solubility.

3.2.2 Al solubility under different weather conditions

We encountered four representative weather conditions (i.e. clean, dust, haze and fog days) during our sampling at Xi'an and Qingdao, and investigated aerosol Al solubility under different weather conditions (Figure 4, Tables S6-S7).

At Xi'an, no apparent difference in Al solubility was observed during clean, haze, and dust days (Figure 4a, Table S6), with median values in the range of 1.01-1.47% for supermicron particles and 0.72-1.86% for submicron particles. Al solubility was found to be <1.2% for three mineral dust samples (Luochuan loess, Arizona test dust, and dust collected during a dust storm in Xinjiang) (Li et al., 2022), and ranged from 0.47% to 1.42% for aerosol particles generated using soil samples from Saharan desert (Shi et al., 2011). Compared to mineral dust in source regions, Al solubility was not higher under different weather conditions at Xi'an. In addition, although emission and accumulation of anthropogenic pollutants was greatly enhanced during haze days at Xi'an (An et al., 2019; Cao and Cui, 2021), there was no obvious increase in

aerosol Al solubility, indicating that the effects of anthropogenic emissions on aerosol Al solubility was limited at Xi'an. Therefore, one may conclude that aerosol Al solubility at Xi'an was not different from initial Al solubility of mineral dust.

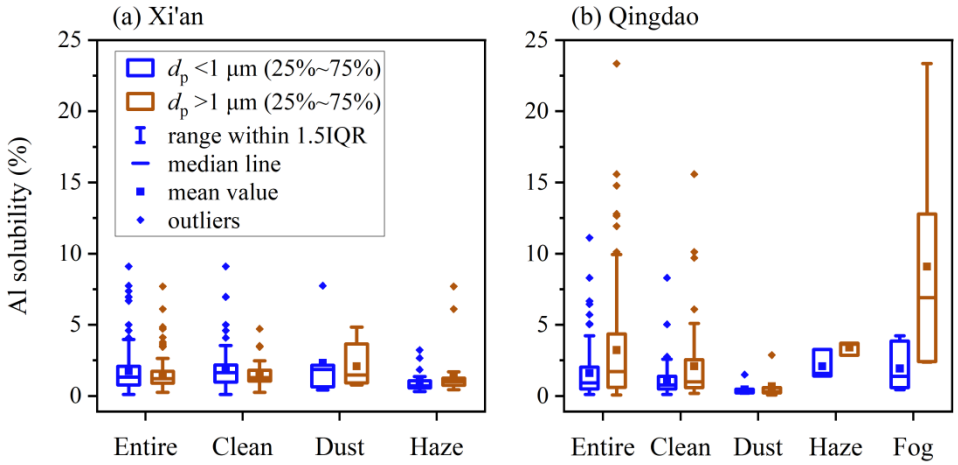

Figure 4. Aerosol Al solubility under different weather conditions for submicron and supermicron particles: (a) Xi'an, (b) Qingdao.

Being different to Xi'an, aerosol Al solubility at Qingdao shows remarkable variations under different weather conditions (Figure 4b, Table S7). Median Al solubilities were determined to be 0.31% and 0.24% for supermicron and submicron particles during dust days, lower than these on clean days (0.99% and 0.77%, respectively). This is probably because higher wind speeds during dust events hindered the accumulation of atmospheric pollutants and shortened the transport time to Qingdao, and thus limiting the aging of mineral dust aerosol. This explanation is supported by a recent study (Zhang et al., 2024) which found that the aging extent of dust particles in Japan was much lower during fast-moving dust events than slow-moving dust events. Moreover, large amounts of alkaline components (such as carbonates) which were emitted to the atmosphere during dust days neutralized acid species and therefore

inhibited acid-promoted dissolution of aerosol trace elements (Zhi et al., 2025). Our work implies that during large dust events increase in aerosol Al solubility may be rather limited when dust is transported to Qingdao; nevertheless, when dust is transported further eastward to the open ocean, atmospheric chemical processing may substantially increase aerosol Al solubility.

Figure 4b also suggests that aerosol Al solubilities were much higher during haze and fog days at Qingdao, when compared to clean days. Highest Al solubilities were observed during fog days, with median values being 6.90% for supermicron particles and 1.38% for submicron particles, followed by haze days (3.64% and 1.58%, respectively). This is very likely due to enhanced chemical processing during haze and fog periods (Shi et al., 2020; Shang et al., 2024), and especially during fog days the large increase in RH cause huge increase in aerosol liquid water, therefore greatly promoting aqueous reactions and Al dissolution. Acid and ligand processing can both enhance aerosol Al solubility, although at present it is difficult to disentangle their individual contributions.

In summary, aerosol Al solubility at Xi'an was low in general, and did not show much variability in different seasons or under different weather conditions. Compared to Xi'an, aerosol Al solubility was higher at Qingdao; furthermore, it was higher in the other three seasons than in spring, and much higher for haze and fog days than dust days. These results imply that atmospheric aging had little effect on aerosol Al solubility at Xi'an but could remarkably increase aerosol Al solubility at Qingdao, as further elaborated in Section 4.

4. Discussion

As shown in Figure 5, our work observed the inverse dependence of aerosol Al solubility on total Al concentrations at both Xi'an and Qingdao, given by Eq. (1):

$$f_s(\mathrm{Al}) = \mathrm{a} \times [\mathrm{Al}]^{-b} \qquad (1)$$

where f_s(Al) is aerosol Al solubility (%) and [Al] is total Al concentration (ng/m^3). Such relationship was also reported in some previous studies (Jickells et al., 2016; Shelley et al., 2018; Baker et al., 2020; Shelley et al., 2025). Baker and Jickells (2006) suggested that such inverse relationship was due to that larger particles have higher deposition velocities and lower Al solubility: aerosol Al concentrations decrease during transport in the atmosphere due to deposition, with deposition being faster for larger particles; as a result, aerosol particles will be enriched with smaller particles with higher Al solubility. However, Shi et al. (2011) found no substantial change in Al solubility with particle size for mineral dust samples, and therefore put the explanation proposed by Baker and Jickells (2006) into doubt.

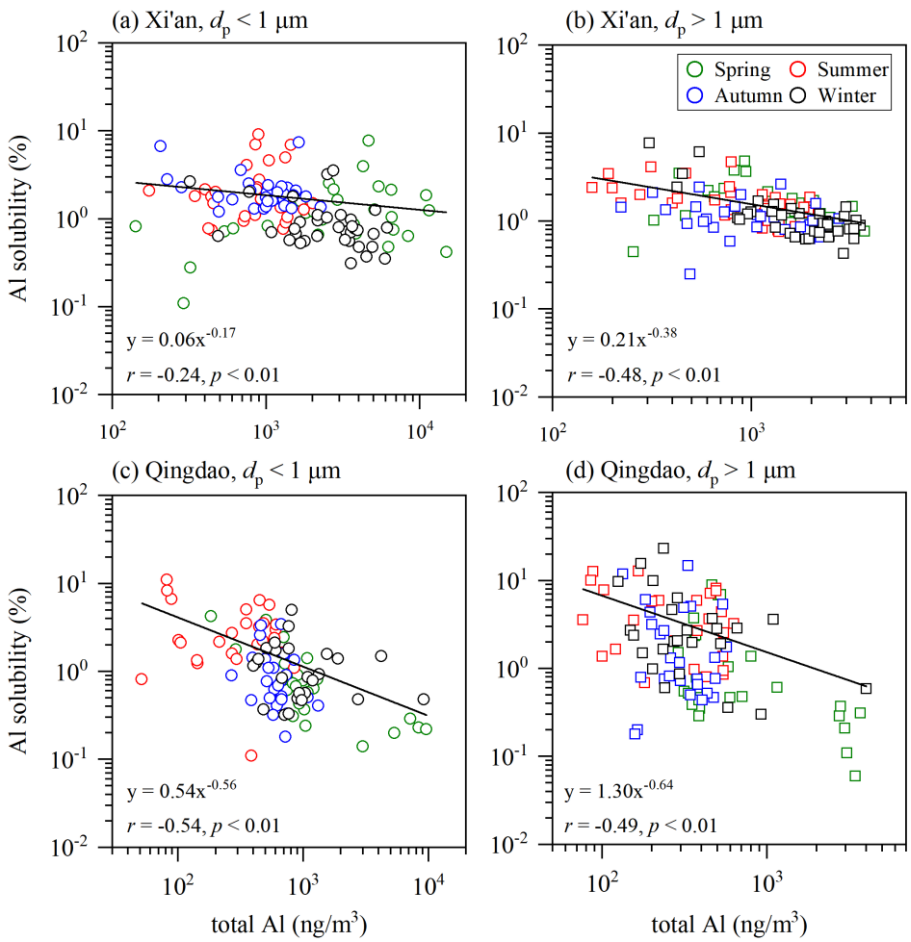

335

336 **Figure 5.** Aerosol Al solubility versus total aerosol Al concentrations: (a) submicron particles
337 at Xi'an, (b) supermicron particles at Xi'an, (c) submicron particles at Qingdao, (d)
338 supermicron particles at Qingdao.

339

340 Aerosol Fe solubility was also frequently observed to increase with the decrease in total
341 Fe concentrations (Sedwick et al., 2007; Mahowald et al., 2018; Meskhidze et al., 2019), and
342 one possible reason is the influence of anthropogenic aerosol Fe (Sholkovitz et al., 2009; Ito
343 and Shi, 2016) with higher solubility than mineral dust (Schroth et al., 2009; Fu et al., 2012;
344 Ito et al., 2021). Nevertheless, being different from aerosol Fe, aerosol Al stems
345 predominantly from mineral dust, with little contribution from anthropogenic sources;

346 furthermore, Al solubility was measured to be 0.4±0.6% for coal fly ash (Li et al., 2022), an
347 important type of anthropogenic aerosols, not higher than that for mineral dust (0.8±0.4%).
348 Therefore, we suggest that anthropogenic emission may not be able to explain the inverse
349 dependence of Al aerosol solubility on total Al concentrations.

350 We argue that chemical processing in the atmosphere can very well explain such inverse
351 dependence. Total aerosol Al concentrations decrease with transport due to deposition, while
352 reactions with acidic gases (such as SO_2 and NO_x) can enhance the dissolution of aerosol Al
353 (Jickells et al., 2016). Figure 5 shows that the inverse dependence of Al solubility on total Al
354 concentration was more pronounced at Qingdao, with the slopes (*b* values) much larger than
355 those obtained at Xi'an. This is because compared to Xi'an, Qingdao is more distant from
356 deserts and therefore dust aerosol is expected to be more aged at Qingdao. It also further
357 supports the vital role chemical aging plays in regulating aerosol Al solubility,

358 **4.1 Effects of acid processing and the role of RH**

359 **4.1.1 Effects of acid processing**

360 Laboratory experiments found that the amount of Al dissolved from minerals would
361 increase with the decrease in solution pH (Amram and Ganor, 2005; Bibi et al., 2011, 2014;
362 Cappelli et al., 2018), and some field measurements also suggested that acid processing in the
363 atmosphere could lead to large increase in aerosol Al solubility (Measures et al., 2010; Sakata
364 et al., 2023). In this work, we examined the relationship between aerosol Al solubility and the
365 relative abundance of acidic species ([sulfate]/[Al] and [nitrate]/[Al]) at Xi'an and Qingdao. It
366 should be noted that non-sea-salts sulfate (Virkkula et al., 2006), instead of sulfate, was used
367 at Qingdao because it is a coastal city and heavily impacted by sea spray aerosol.

At Xi'an, overall aerosol Al solubility showed no significant correlation with [sulfate]/[Al] or [nitrate]/[Al] for either supermicron or submicron particles (r < 0.4, Figure 6 and S1), indicating that acid processing did not enhance aerosol Al solubility. Enhancement of aerosol trace element solubility by acid processing requires internal mixing of acid species with mineral dust particles (Baker and Croot, 2010). Previous studies suggested that mineral dust particles observed at Xi'an which is close to deserts largely remained externally mixed with acid species (Wang et al., 2014; Wu et al., 2017), and thus aerosol Al solubility was not apparently enhanced by acid processing at Xi'an.

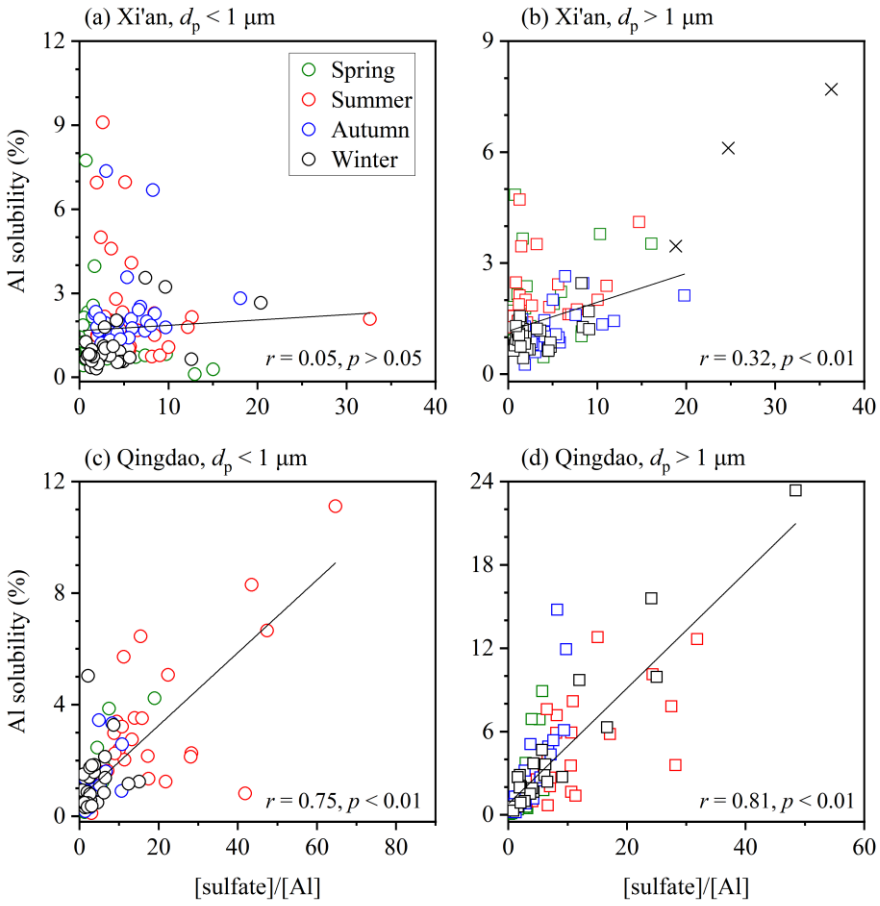

Figure 6. Aerosol Al solubility versus [sulfate]/[Al]: (a) submicron particles at Xi'an, (b) supermicron particles at Xi'an, (c) submicron particles at Qingdao, (d) supermicron particles

at Qingdao (the *r* value changed from 0.81 to 0.74 if the data point with the highest Al solubility was excluded). Data represented by crosses are not included in fitting.

On the contrary, Figure 6 shows that aerosol Al solubility at Qingdao was well correlated with [sulfate]/[Al] ($r > 0.7$, $p < 0.01$), implying that acidic species were internally mixed with mineral dust particles and thus acid-promoted dissolution significantly enhanced Al solubility. We also found that correlations of Al solubility with [sulfate]/[Al] was better than those with [nitrate]/[Al] (Figures 6 and S1, Table S8), in line with a previous study (Sakata et al., 2023) which found aerosol Al solubility at Hiroshima, southern Japan, to be correlated with [sulfate]/[Al] but not with [nitrate]/[Al]. This may imply that chemical processing by sulfate was more important than nitrate for Al solubility enhancement via acid processing, likely because aluminosilicate dust particles tend to react preferentially with SO_2 and H_2SO_4 while nitrogen oxides react mainly with carbonate particles (Sullivan et al., 2007; Fitzgerald et al., 2015). Furthermore, our work reveals better correlations between Al solubility and [sulfate]/[Al] for supermicron particles than submicron particles (Figure 6), indicating that the effect of acid processing on Al solubility was more important in supermicron particles.

4.1.2 The role of RH

Relative humidity (RH) is a vital factor influencing liquid water contents and phase state of aerosol particles and thus their secondary chemistry. When RH increased >60%, the phase state of aerosol particles in Northern China changed from semisolid to liquid (Liu et al., 2017; Sun et al., 2018; Song et al., 2022), leading to large increase in aerosol liquid water content and thereby potentially affecting aerosol Al solubility.

We observed no apparent variation of aerosol Al solubility with RH at Xi'an (Figure 7a). When RH was <60%, median Al solubilities for supermicron and submicron particles were 1.22% and 1.14%, respectively; when RH increased >90%, the median Al solubilities were determined to be 1.82% and 0.82%, showing no obvious increase when compared to those at <60% RH. This again may imply that chemical processing had very limited impact on aerosol Al solubility at Xi'an, as mineral dust particles mostly remained externally mixed with secondary species and their aging extent was very limited (Wang et al., 2014; Wu et al., 2017).

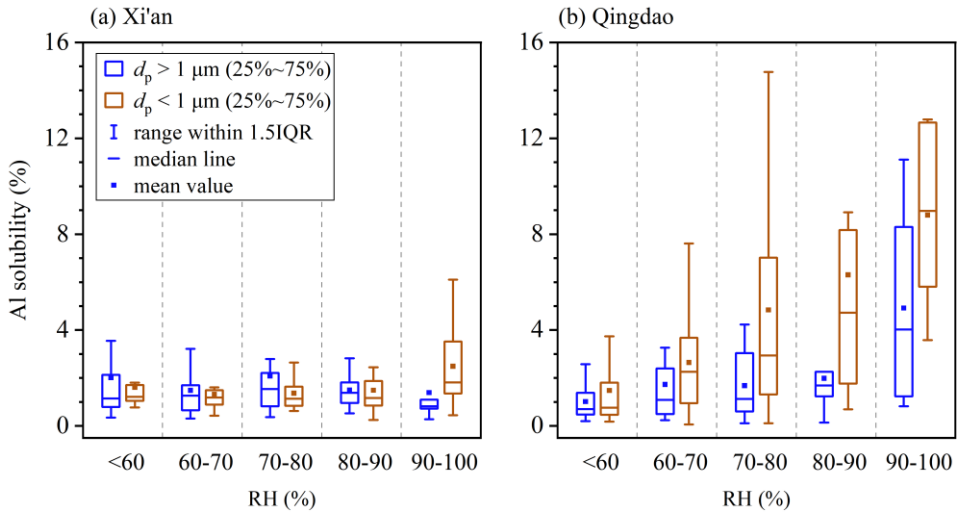

Figure 7. Aerosol Al solubility at different relative humidity (RH) for submicron and supermicron particles: (a) Xi'an, (b) Qingdao.

In contrast, RH played an important role in regulating aerosol Al solubility at Qingdao, because mineral dust particles observed at Qingdao had been transported through the North China Plain and were substantially aged. As shown in Figure 7b, for supermicron particles, the median Al solubility was only 0.76% at <60% RH, and gradually increased to 4.73% at 80-90% RH, and abruptly increased to 8.87% at >90% RH. For submicron particles, median Al

solubility was <1% at <60% RH, and further increase in RH to 80-90% did not lead to large changes in Al solubility; nevertheless, when RH exceeded 90%, the median Al solubility was remarkably increased to 4.02%, much higher than those observed when RH was < 90%.

4.2 Effects of aerosol acidity on aerosol Al solubility at Qingdao

Figure 8 shows the dependence of aerosol Al solubility on aerosol acidity (represented by pH) at Qingdao (we did not measure NH_3 at Xi'an and thus could not estimate the aerosol acidity in a reliable manner). For supermicron particles, the median Al solubility was only 0.99% when aerosol pH was >4.0, and gradually increased to 10.24% as aerosol pH was decreased to <2.5. For submicron particles, the median Al solubility was only 0.69% when pH was >4.0, increased slightly with the decrease in pH when pH was in the range of 2.5-4.0, and then increased greatly to 6.09% when pH was decreased to <2.5. In addition, aerosol acidity at Qingdao was highest in summer and lowest in spring (Chen et al., 2024), consistent with the seasonal variation of aerosol Al solubility, further supporting the importance of aerosol acidity in regulating Al solubility.

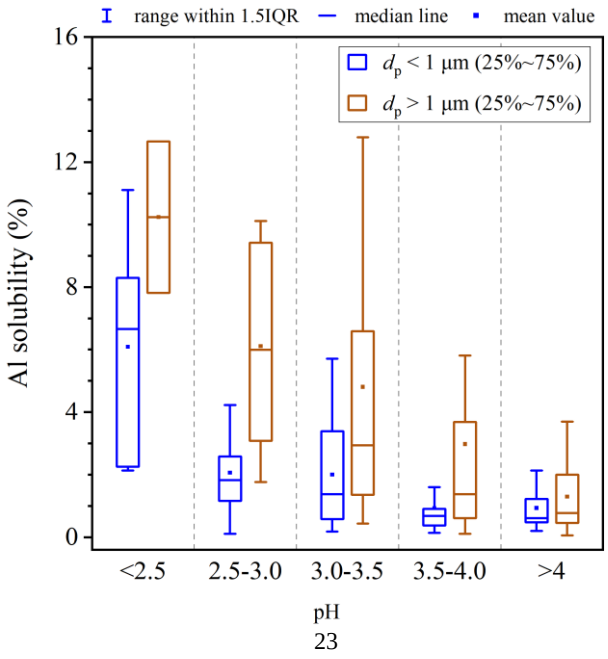

Figure 8. Aerosol Al solubility corresponding to different aerosol acidity for submicron and supermicron particles in Qingdao.

As shown in Figure S2, aerosol Al solubility was generally <2% when aerosol acidity was low (pH > 4.0), and higher Al solubility (>2%) was usually observed for samples with high RH and high acidity (pH < 4.0), again underscoring the roles of aerosol acidity (and RH). However, some samples exhibited low Al solubility although the corresponding RH and aerosol acidity were both higher, and such phenomenon was more pronounced for submicron particles. This is very likely linked with aerosol mixing state (Riemer et al., 2019). Aerosol Al solubility and acidity used in our work are both the average properties of an aerosol sample which contains numerous particles, while in reality the two properties will have large particle-to-particle variations. For a given aerosol sample, it can happen that particles with high acidity may contain very little Al while particles with low acidity are enriched in Al; in this case, high acidity do not promote Al solubility for this sample. Single particle analysis which provides mixing state information can give further insights. We also note that samples with low Al solubility but high RH and high acidity were mostly found in clean days, perhaps due to the influence of local resuspended dust for which chemical aging was very limited.

4.3 Size-dependence of aerosol Al solubility

At Xi'an, no obvious difference in aerosol Al solubility was found between supermicron and submicron particles across all the four seasons (Figure 3a). This is because the aging extent of dust particles was rather limited at Xi'an (Wang et al., 2014; Wu et al., 2017) and Al solubility does not vary with particle size for unaged dust particles (Shi et al., 2011). At

Qingdao, aerosol Al solubility showed no obvious difference between supermicron and submicron particles in spring, because the aging extent of dust arriving at Qingdao was also limited in spring when Asian dust occurred most frequently. However, in the other three seasons, Al solubility was higher for supermicron particles than submicron particles at Qingdao, and the ratios of median Al solubility in supermicron particles to that in submicron particles were found to be 1.53, 1.70 and 2.57 in summer, autumn and winter, respectively. Similar to our observation at Qingdao, Li et al. (2017) found that aerosol Al solubility was much higher for TSP (14-28%) than $PM_{2.5}$ (2-23%) at the summit of Mount Heng, southern China.

On the other hand, a few other studies (Baker et al., 2020; Hsieh et al., 2023; Sakata et al., 2023; Yang et al., 2023) found that aerosol Al solubility was higher in fine particles than coarse particles. For example, aerosol Al solubility was found to increase with the decrease in particle size over the tropical eastern Atlantic (Baker et al., 2020), being ~10.31% for particles in the size of 0.36-0.61 μm and 0.43-4.53% for particles above 0.61 μm. At Hiroshima, southern Japan, aerosol Al solubility was reported to be 8.82±6.48% for fine particles (<1.3 μm), more than two times larger than that (3.25±3.41%) for coarse particles (>1.3 μm) (Sakata et al., 2023). Baker and Jickells (2006) suggested that this is because fine particles have larger surface-to-volume ratios and thus facilitate Al dissolution via acid processing. Hsieh et al. (2023) found aerosol Al solubility to be 38% for fine particles (0.57-1.0 μm) but only 0.37% for coarse particles (>7.3 μm) over the East China Sea, and suggested that the observed size-dependence could be explained by the enrichment of anthropogenic Al (which has higher solubility than dust Al) in fine particles. However, aerosol Al originates predominantly from mineral dust, with little contribution from anthropogenic sources (Taylor and McLennan, 1985; Mahowald

et al., 2018), and fractional solubility of anthropogenic Al was not necessarily higher than mineral dust (Li et al., 2022).

As discussed above, there is not clear yet how and why aerosol Al solubility varies with particle size. Such discrepancy is at least partly because different leaching protocols were used in previous studies to extract dissolved aerosol Al and thereby Al solubility obtained in different studies was not directly comparable (Meskhidze et al., 2019; Li et al., 2023; Li et al., 2024). Furthermore, mechanistic insights can be obtained by laboratory experiments which examine the size dependence of the solubility and dissolution kinetics of Al for mineral dust particles under atmospherically relevant conditions.

5. Conclusions and atmospheric implications

Deposition of mineral dust aerosol is a major external source of several nutrient and toxic elements for surface water in open oceans, and thus have large impacts on marine biogeochemistry; however, previous studies which estimated dust deposition flux into the oceans reveals large discrepancies. Aerosol Al solubility, which is a critical parameter in using dissolved Al concentrations in surface seawater as a tracer to constrain dust deposition flux, remains poorly understood. In this work, we investigated seasonal variations of aerosol Al solubility for supermicron (>1 μm) and submicron (<1 μm) aerosol particles at Xi'an and Qingdao, both located in Northern China, in attempt to elucidate the processes and mechanisms which govern the variation of aerosol Al solubility in the atmosphere.

At Xi'an, aerosol Al solubility was low in general for both supermicron and submicron particles, showing no obvious variability in different seasons or under different weather conditions. This implies that chemical processing did not substantially enhance aerosol Al

499 solubility at Xi'an, as it is an inland city close to major deserts in Northwestern China and thus
500 the aging extent of mineral dust particles arriving at Xi'an was quite limited. Compared to
501 Xi'an, aerosol Al solubility was higher at Qingdao, a coastal city in Northern China;
502 furthermore, Al solubility was higher in the other three seasons than in spring, and much higher
503 for haze- and especially fog-impacted days than dust days. This indicates that chemical
504 processing substantially increased aerosol Al solubility at Qingdao.

505 Aerosol Al solubility at Xi'an showed no significant correlation with relative abundance
506 of sulfate or nitrate, and did not vary apparently with RH; in contrast, Al solubility at Qingdao
507 was well correlated with relative abundance of sulfate and nitrate, and increased with RH. This
508 further supports that chemical processing had little impact on aerosol Al solubility at Xi'an
509 (because the aging extent of mineral dust aerosol at Xi'an is very limited) but remarkably
510 increased aerosol Al solubility at Qingdao (because mineral dust particles transported to
511 Qingdao were substantially aged). Moreover, for both supermicron and submicron particles,
512 Al solubility at Qingdao was found to increase with aerosol acidity (in addition to RH),
513 underscoring the vital role of aerosol liquid water and acidity in enhancing Al dissolution via
514 chemical aging.

515 Our comprehensive investigation of aerosol Al solubility at two locations in Northern
516 China suggests that atmospheric chemical processing dictates aerosol Al solubility. As a result,
517 aerosol Al solubility is expected to spatially variable, depending on the extent of chemical
518 processing. For example, we found that aerosol Al solubility is higher at Qingdao than Xi'an
519 in general, and expect it to increase further as mineral dust aerosol is further transported
520 eastward to the Pacific. Although our measurements were only conducted at two sites, our work

provides important insights into processes driving spatiotemporal variability of aerosol Al solubility, and such understanding can aid us to develop aerosol Al solubility parameterizations.

Author contribution.

TZ: Formal analysis, Investigation, Writing - Original Draft, Writing - Review & Editing; **YC:** Formal analysis, Investigation, Writing - Original Draft; **HZ:** Investigation; **Lei Liu:** Writing - Review & Editing; **CH:** Investigation; **ZF:** Investigation; **YZ:** Investigation; **FW:** Resources; **Lan Luo:** Resources; **GZ:** Writing - Review & Editing; **XW:** Resources; **MT:** Conceptualization, Formal analysis, Supervision; Writing - Original Draft, Writing - Review & Editing.

Competing interests.

The authors declare that they have no conflict of interest.

Acknowledgement.

We would like to thank colleagues at Shandong University, Shaanxi University of Science and Technology, and Institute of Earth Environment, Chinese Academy of Sciences for their support during field measurements.

Financial support.

This work was sponsored by National Natural Science Foundation of China (42277088, 42407149 and 22361162668), Guangzhou Bureau of Science and Technology (2024A04J6533), International Partnership Program of Chinese Academy of Sciences (164GJHZ2024011FN), Guangdong Basic and Applied Basic Research Fund Committee

(2023A1515012010), and Guangdong Foundation for Program of Science and Technology Research (2023B1212060049).

References

Aghnatios, C., Losno, R., and Dulac, F.: A fine fraction of soil used as an aerosol analogue during the DUNE experiment: sequential solubility in water, decreasing pH step-by-step, Biogeosciences, 11, 4627-4633, https://doi.org/10.5194/bg-11-4627-2014, 2014.

Amram, K., and Ganor, J.: The combined effect of pH and temperature on smectite dissolution rate under acidic conditions, Geochim. Cosmochim. Acta, 69, 2535-2546, https://doi.org/10.1016/j.gca.2004.10.001, 2005.

An, Z., Huang, R., Zhang, R., Tie, X., Li, G., Cao, J., Zhou, W., Shi, Z., Han, Y., Gu, Z., and Ji, Y.: Severe haze in northern China: A synergy of anthropogenic emissions and atmospheric processes, PNAS, 116, 8657-8666, https://doi.org/10.1073/pnas.1900125116, 2019.

Anderson, R. F., Cheng, H., Edwards, R. L., Fleisher, M. Q., Hayes, C. T., Huang, K. F., Kadko, D., Lam, P. J., Landing, W. M., Lao, Y., Lu, Y., Measures, C. I., Moran, S. B., Morton, P. L., Ohnemus, D. C., Robinson, L. F., and Shelley, R. U.: How well can we quantify dust deposition to the ocean?, Phil. Trans. R. Soc. A, 374: 20150285, https://doi.org/10.1098/rsta.2015.0285, 2016.

Baker, A. R., and Jickells, T. D.: Mineral particle size as a control on aerosol iron solubility, Geophys. Res. Lett., 33, L17608, https://doi.org/10.1029/2006gl026557, 2006.

Baker, A. R., Jickells, T. D., Witt, M., and Linge, K. L.: Trends in the solubility of iron, aluminium, manganese and phosphorus in aerosol collected over the Atlantic Ocean, Mar. Chem., 98, 43-58, https://doi.org/10.1016/j.marchem.2005.06.004, 2006.

Baker, A. R., and Croot, P. L.: Atmospheric and marine controls on aerosol iron solubility in seawater, Mar. Chem., 120, 4-13, https://doi.org/10.1016/j.marchem.2008.09.003, 2010.

Baker, A. R., Li, M., and Chance, R.: Trace Metal Fractional Solubility in Size‐Segregated Aerosols From the Tropical Eastern Atlantic Ocean, Global Biogeochem. Cycles, 34, e2019GB006510, https://doi.org/10.1029/2019gb006510, 2020.

Benaltabet, T., Lapid, G., and Torfstein, A.: Dissolved aluminium dynamics in response to dust storms, wet deposition, and sediment resuspension in the Gulf of Aqaba, northern Red Sea, Geochim. Cosmochim. Acta, 335, 137-154, https://doi.org/10.1016/j.gca.2022.08.029, 2022.

Bibi, I., Singh, B., and Silvester, E.: Dissolution of illite in saline–acidic solutions at 25°C, Geochim. Cosmochim. Acta, 75, 3237-3249, https://doi.org/10.1016/j.gca.2011.03.022, 2011.

Bibi, I., Singh, B., and Silvester, E.: Dissolution kinetics of soil clays in sulfuric acid solutions: Ionic strength and temperature effects, Appl. Geochem., 51, 170-183, https://doi.org/10.1016/j.apgeochem.2014.10.004, 2014.

Buck, C. S., Landing, W. M., Resing, J. A., and Measures, C. I.: The solubility and deposition of aerosol Fe and other trace elements in the North Atlantic Ocean: Observations from the A16N CLIVAR/CO2 repeat hydrography section, Mar. Chem., 120, 57-70, https://doi.org/10.1016/j.marchem.2008.08.003, 2010.

Buck, C. S., Landing, W. M., and Resing, J.: Pacific Ocean aerosols: Deposition and solubility of iron, aluminum, and other trace elements, Mar. Chem., 157, 117-130, https://doi.org/10.1016/j.marchem.2013.09.005, 2013.

Cai, Q.-L., Dai, X.-R., Li, J.-R., Tong, L., Hui, Y., Cao, M.-Y., Li, M., and Xiao, H.: The characteristics and mixing states of PM2.5 during a winter dust storm in Ningbo of the Yangtze River Delta, China, Sci. Total Environ., 709, 136146, https://doi.org/10.1016/j.scitotenv.2019.136146, 2020.

Cao, J. J., Chow, J. C., Watson, J. G., Wu, F., Han, Y. M., Jin, Z. D., Shen, Z. X., and An, Z. S.: Size-

differentiated source profiles for fugitive dust in the Chinese Loess Plateau, Atmos. Environ., 42, 2261-2275, https://doi.org/10.1016/j.atmosenv.2007.12.041, 2008.

Cao, J. J., and Cui, L.: Current Status, Characteristics and Causes of Particulate Air Pollution in the Fenwei Plain, China: A Review, J. Geophys. Res.-Atmos., 126, e2020JD034472, https://doi.org/10.1029/2020JD034472, 2021.

Cappelli, C., Yokoyama, S., Cama, J., and Huertas, F. J.: Montmorillonite dissolution kinetics: Experimental and reactive transport modeling interpretation, Geochim. Cosmochim. Acta, 227, 96-122, https://doi.org/10.1016/j.gca.2018.01.039, 2018.

Chance, R., Jickells, T. D., and Baker, A. R.: Atmospheric trace metal concentrations, solubility and deposition fluxes in remote marine air over the south-east Atlantic, Mar. Chem., 177, 45-56, https://doi.org/10.1016/j.marchem.2015.06.028, 2015.

Chen, Y., Wang, Z., Fang, Z., Huang, C., Xu, H., Zhang, H., Zhang, T., Wang, F., Luo, L., Shi, G., Wang, X., and Tang, M.: Dominant Contribution of Non-dust Primary Emissions and Secondary Processes to Dissolved Aerosol Iron, Environ. Sci. Technol., 58, 17355-17363, https://doi.org/10.1021/acs.est.4c05816, 2024.

Duvall, R. M., Majestic, B. J., Shafer, M. M., Chuang, P. Y., Simoneit, B. R. T., and Schauer, J. J.: The water-soluble fraction of carbon, sulfur, and crustal elements in Asian aerosols and Asian soils, Atmos. Environ., 42, 5872-5884, https://doi.org/10.1016/j.atmosenv.2008.03.028, 2008.

Fang, Z., Dong, S., Huang, C., Jia, S., Wang, F., Liu, H., Meng, H., Luo, L., Chen, Y., Zhang, H., Li, R., Zhu, Y., and Tang, M.: On using an aerosol thermodynamic model to calculate aerosol acidity of coarse particles, J. Environ. Sci., 148, 46-56, https://doi.org/10.1016/j.jes.2023.07.001, 2025.

Fitzgerald, E., Ault, A. P., Zauscher, M. D., Mayol-Bracero, O. L., and Prather, K. A.: Comparison of the mixing state of long-range transported Asian and African mineral dust, Atmos. Environ., 115, 19-25, https://doi.org/10.1016/j.atmosenv.2015.04.031, 2015.

Fountoukis, C., and Nenes, A.: ISORROPIA II: a computationally efficient thermodynamic equilibrium model for K^+-Ca^{2+}-Mg^{2+}-NH_4^+-Na^+-SO_4^{2-}-NO_3^--Cl^--H_2O aerosols, Atmos. Chem. Phys., 7, 4639-4659, https://doi.org/10.5194/acp-7-4639-2007, 2007.

Fu, H., Lin, J., Shang, G., Dong, W., Grassian, V. H., Carmichael, G. R., Li, Y., and Chen, J.: Solubility of Iron from Combustion Source Particles in Acidic Media Linked to Iron Speciation, Environ. Sci. Technol., 46, 11119-11127, https://doi.org/10.1021/es302558m, 2012.

Grand, M. M., Measures, C. I., Hatta, M., Hiscock, W. T., Buck, C. S., and Landing, W. M.: Dust deposition in the eastern Indian Ocean: The ocean perspective from Antarctica to the Bay of Bengal, Global Biogeochem. Cycles, 29, 357-374, https://doi.org/10.1002/2014GB004898, 2015.

Guo, L., Chen, Y., Wang, F., Meng, X., Xu, Z., and Zhuang, G.: Effects of Asian dust on the atmospheric input of trace elements to the East China Sea, Mar. Chem., 163, 19-27, https://doi.org/10.1016/j.marchem.2014.04.003, 2014.

Han, Q., Moore, J. K., Zender, C., Measures, C., and Hydes, D.: Constraining oceanic dust deposition using surface ocean dissolved Al, Global Biogeochem. Cycles, 22, GB2003, https://doi.org/10.1029/2007GB002975, 2008.

Haugvaldstad, O. W., Tang, H., Kaakinen, A., Bohm, K., Groot Zwaaftink, C. D., Grythe, H., Stevens, T., Zhang, Z., and Stordal, F.: Spatial Source Contribution and Interannual Variation in Deposition of Dust Aerosols Over the Chinese Loess Plateau, J. Geophys. Res.-Atmos., 129, e2023JD040470, https://doi.org/10.1029/2023JD040470, 2024.

631 Hsieh, C.-C., You, C.-F., and Ho, T.-Y.: The solubility and deposition flux of East Asian aerosol metals in the
632 East China Sea: The effects of aeolian transport processes, Mar. Chem., 253, 104268,
633 https://doi.org/10.1016/j.marchem.2023.104268, 2023.
634 Hsu, S.-C., Wong, G. T. F., Gong, G.-C., Shiah, F.-K., Huang, Y.-T., Kao, S.-J., Tsai, F., Candice Lung, S.-C.,
635 Lin, F.-J., Lin, I. I., Hung, C.-C., and Tseng, C.-M.: Sources, solubility, and dry deposition of aerosol
636 trace elements over the East China Sea, Mar. Chem., 120, 116-127,
637 https://doi.org/10.1016/j.marchem.2008.10.003, 2010.
638 Huang, R.-J., Zhang, Y., Bozzetti, C., Ho, K.-F., Cao, J.-J., Han, Y., Daellenbach, K. R., Slowik, J. G., Platt, S.
639 M., Canonaco, F., Zotter, P., Wolf, R., Pieber, S. M., Bruns, E. A., Crippa, M., Ciarelli, G., Piazzalunga,
640 A., Schwikowski, M., Abbaszade, G., Schnelle-Kreis, J., Zimmermann, R., An, Z., Szidat, S.,
641 Baltensperger, U., Haddad, I. E., and Prévôt, A. S. H.: High secondary aerosol contribution to
642 particulate pollution during haze events in China, Nature, 514, 218-222, 10.1038/nature13774, 2014.
643 Huneeus, N., Schulz, M., Balkanski, Y., Griesfeller, J., Prospero, J., Kinne, S., Bauer, S., Boucher, O., Chin, M.,
644 Dentener, F., Diehl, T., Easter, R., Fillmore, D., Ghan, S., Ginoux, P., Grini, A., Horowitz, L., Koch, D.,
645 Krol, M. C., Landing, W., Liu, X., Mahowald, N., Miller, R., Morcrette, J. J., Myhre, G., Penner, J.,
646 Perlwitz, J., Stier, P., Takemura, T., and Zender, C. S.: Global dust model intercomparison in AeroCom
647 phase I, Atmos. Chem. Phys., 11, 7781-7816, https://doi.org/10.5194/acp-11-7781-2011, 2011.
648 Ito, A., and Shi, Z.: Delivery of anthropogenic bioavailable iron from mineral dust and combustion aerosols to
649 the ocean, Atmos. Chem. Phys., 16, 85-99, https://doi.org/10.5194/acp-16-85-2016, 2016.
650 Ito, A., Ye, Y., Baldo, C., and Shi, Z.: Ocean fertilization by pyrogenic aerosol iron, npj Clim. Atmos. Sci., 4, 30,
651 https://doi.org/10.1038/s41612-021-00185-8, 2021.
652 Jeong, G. Y.: Mineralogy and geochemistry of Asian dust: dependence on migration path, fractionation, and
653 reactions with polluted air, Atmos. Chem. Phys., 20, 7411-7428, https://doi.org/10.5194/acp-20-7411-
654 2020, 2020.
655 Jiang, H.-B., Hutchins, D. A., Zhang, H.-R., Feng, Y.-Y., Zhang, R.-F., Sun, W.-W., Ma, W., Bai, Y., Wells, M.,
656 He, D., Jiao, N., Wang, Y., and Chai, F.: Complexities of regulating climate by promoting marine
657 primary production with ocean iron fertilization, Earth Sci. Rev., 249, 104675,
658 https://doi.org/10.1016/j.earscirev.2024.104675, 2024.
659 Jickells, T. D., An, Z. S., Andersen, K. K., Baker, A. R., Bergametti, G., Brooks, N., Cao, J. J., Boyd, P. W.,
660 Duce, R. A., Hunter, K. A., Kawahata, H., Kubilay, N., laRoche, J., Liss, P. S., Mahowald, N.,
661 Prospero, J. M., Ridgwell, A. J., Tegen, I., and Torres, R.: Global Iron Connections Between Desert
662 Dust, Ocean Biogeochemistry, and Climate, Science, 308, 67-71,
663 https://doi.org/10.1126/science.1105959, 2005.
664 Jickells, T. D., Baker, A. R., and Chance, R.: Atmospheric transport of trace elements and nutrients to the
665 oceans, Phil. Trans. R. Soc. A, 374, 20150286, https://doi.org/10.1098/rsta.2015.0286, 2016.
666 Kok, J. F., Storelvmo, T., Karydis, V. A., Adebiyi, A. A., Mahowald, N. M., Evan, A. T., He, C., and Leung, D.
667 M.: Mineral dust aerosol impacts on global climate and climate change, Nat. Rev. Earth Environ., 4,
668 71-86, https://doi.org/10.1038/s43017-022-00379-5, 2023.
669 Li, R., Zhang, H., Wang, F., Ren, Y., Jia, S., Jiang, B., Jia, X., Tang, Y., and Tang, M.: Abundance and fractional
670 solubility of phosphorus and trace metals in combustion ash and desert dust: Implications for
671 bioavailability and reactivity, Sci. Total Environ., 816, 151495,
672 https://doi.org/10.1016/j.scitotenv.2021.151495, 2022.
673 Li, R., Dong, S., Huang, C., Yu, F., Wang, F., Li, X., Zhang, H., Ren, Y., Guo, M., Chen, Q., Ge, B., and Tang,

M.: Evaluating the effects of contact time and leaching solution on measured solubilities of aerosol trace metals, Appl. Geochem., 148, 105551, https://doi.org/10.1016/j.apgeochem.2022.105551, 2023.

Li, R., Panda, P. P., Chen, Y., Zhu, Z., Wang, F., Zhu, Y., Meng, H., Ren, Y., Kumar, A., and Tang, M.: Aerosol trace element solubility determined using ultrapure water batch leaching: an intercomparison study of four different leaching protocols, Atmos. Meas. Tech., 17, 3147-3156, https://doi.org/10.5194/amt-17-3147-2024, 2024.

Li, T., Wang, Y., Zhou, J., Wang, T., Ding, A., Nie, W., Xue, L., Wang, X., and Wang, W.: Evolution of trace elements in the planetary boundary layer in southern China: Effects of dust storms and aerosol-cloud interactions, J. Geophys. Res.-Atmos., 122, 3492-3506, https://doi.org/10.1002/2016JD025541, 2017.

Li, W., Shao, L., Shi, Z., Chen, J., Yang, L., Yuan, Q., Yan, C., Zhang, X., Wang, Y., Sun, J., Zhang, Y., Shen, X., Wang, Z., and Wang, W.: Mixing state and hygroscopicity of dust and haze particles before leaving Asian continent, J. Geophys. Res.-Atmos., 119, 1044-1059, https://doi.org/10.1002/2013JD021003, 2014.

Liu, Y., Wu, Z., Wang, Y., Xiao, Y., Gu, F., Zheng, J., Tan, T., Shang, D., Wu, Y., Zeng, L., Hu, M., Bateman, A. P., and Martin, S. T.: Submicrometer Particles Are in the Liquid State during Heavy Haze Episodes in the Urban Atmosphere of Beijing, China, Environ. Sci. Technol. Lett., 4, 427-432, https://doi.org/10.1021/acs.estlett.7b00352, 2017.

López-García, P., Gelado-Caballero, M. D., Collado-Sánchez, C., and Hernández-Brito, J. J.: Solubility of aerosol trace elements: Sources and deposition fluxes in the Canary Region, Atmos. Environ., 148, 167-174, https://doi.org/10.1016/j.atmosenv.2016.10.035, 2017.

Mahowald, N.: Aerosol Indirect Effect on Biogeochemical Cycles and Climate, Science, 334, 794-796, https://doi.org/10.1126/science.1207374, 2011.

Mahowald, N. M., Hamilton, D. S., Mackey, K. R. M., Moore, J. K., Baker, A. R., Scanza, R. A., and Zhang, Y.: Aerosol trace metal leaching and impacts on marine microorganisms, Nat. Commun., 9, 2614, https://doi.org/10.1038/s41467-018-04970-7, 2018.

Measures, C. I., and Brown, E. T.: Estimating Dust Input to the Atlantic Ocean Using Surface Water Aluminium Concentrations, in: The Impact of Desert Dust Across the Mediterranean, edited by: Guerzoni, S., and Chester, R., Springer Netherlands, Dordrecht, 301-311, 1996.

Measures, C. I., and Vink, S.: On the use of dissolved aluminum in surface waters to estimate dust deposition to the ocean, Global Biogeochem. Cycles, 14, 317-327, https://doi.org/10.1029/1999GB001188, 2000.

Measures, C. I., Sato, T., Vink, S., Howell, S., and Li, Y. H.: The fractional solubility of aluminium from mineral aerosols collected in Hawaii and implications for atmospheric deposition of biogeochemically important trace elements, Mar. Chem., 120, 144-153, https://doi.org/10.1016/j.marchem.2009.01.014, 2010.

Meskhidze, N., Völker, C., Al-Abadleh, H. A., Barbeau, K., Bressac, M., Buck, C., Bundy, R. M., Croot, P., Feng, Y., Ito, A., Johansen, A. M., Landing, W. M., Mao, J., Myriokefalitakis, S., Ohnemus, D., Pasquier, B., and Ye, Y.: Perspective on identifying and characterizing the processes controlling iron speciation and residence time at the atmosphere-ocean interface, Mar. Chem., 217, 103704, https://doi.org/10.1016/j.marchem.2019.103704, 2019.

Moore, C. M., Mills, M. M., Arrigo, K. R., Berman-Frank, I., Bopp, L., Boyd, P. W., Galbraith, E. D., Geider, R. J., Guieu, C., Jaccard, S. L., Jickells, T. D., La Roche, J., Lenton, T. M., Mahowald, N. M., Marañón, E., Marinov, I., Moore, J. K., Nakatsuka, T., Oschlies, A., Saito, M. A., Thingstad, T. F., Tsuda, A., and Ulloa, O.: Processes and patterns of oceanic nutrient limitation, Nature Geoscience, 6, 701-710,

https://doi.org/10.1038/ngeo1765, 2013.
Mulder, J., van Breemen, N., and Eijck, H. C.: Depletion of soil aluminium by acid deposition and implications for acid neutralization, Nature, 337, 247-249, 10.1038/337247a0, 1989.
Pan, X., Uno, I., Wang, Z., Nishizawa, T., Sugimoto, N., Yamamoto, S., Kobayashi, H., Sun, Y., Fu, P., Tang, X., and Wang, Z.: Real-time observational evidence of changing Asian dust morphology with the mixing of heavy anthropogenic pollution, Sci. Rep., 7, 335, https://doi.org/10.1038/s41598-017-00444-w, 2017.
Paris, R., Desboeufs, K. V., Formenti, P., Nava, S., and Chou, C.: Chemical characterisation of iron in dust and biomass burning aerosols during AMMA-SOP0/DABEX: implication for iron solubility, Atmos. Chem. Phys., 10, 4273-4282, https://doi.org/10.5194/acp-10-4273-2010, 2010.
Prospero, J. M., Ginoux, P., Torres, O., Nicholson, S. E., and Gill, T. E.: Environmental characterization of global sources of atmospheric soil dust identified with the Nimbus 7 Total Ozone Mapping Spectrometer (TOMS) absorbing aerosol product, Rev. Geophys., 40, 2-1-2-31, https://doi.org/10.1029/2000RG000095, 2002.
Riemer, N., Ault, A. P., West, M., Craig, R. L., and Curtis, J. H.: Aerosol Mixing State: Measurements, Modeling, and Impacts, Rev. Geophys., 57, 187-249, https://doi.org/10.1029/2018RG000615, 2019.
Sakata, K., Sakaguchi, A., Yamakawa, Y., Miyamoto, C., Kurisu, M., and Takahashi, Y.: Measurement report: Stoichiometry of dissolved iron and aluminum as an indicator of the factors controlling the fractional solubility of aerosol iron – results of the annual observations of size-fractionated aerosol particles in Japan, Atmos. Chem. Phys., 23, 9815-9836, https://doi.org/10.5194/acp-23-9815-2023, 2023.
Schroth, A. W., Crusius, J., Sholkovitz, E. R., and Bostick, B. C.: Iron solubility driven by speciation in dust sources to the ocean, Nature Geoscience, 2, 337-340, https://doi.org/10.1038/ngeo501, 2009.
Schulz, M., Prospero, J. M., Baker, A. R., Dentener, F., Ickes, L., Liss, P. S., Mahowald, N. M., Nickovic, S., García-Pando, C. P., Rodríguez, S., Sarin, M., Tegen, I., and Duce, R. A.: Atmospheric Transport and Deposition of Mineral Dust to the Ocean: Implications for Research Needs, Environ. Sci. Technol., 46, 10390-10404, https://doi.org/10.1021/es300073u, 2012.
Sedwick, P. N., Sholkovitz, E. R., and Church, T. M.: Impact of anthropogenic combustion emissions on the fractional solubility of aerosol iron: Evidence from the Sargasso Sea, Geochem. Geophys. Geosyst., 8, https://doi.org/10.1029/2007GC001586, 2007.
Shang, T., Kong, L., and Qi, J.: Metal elements in atmospheric aerosols during different pollution events in the coastal region of the Yellow Sea: Concentration, solubility and deposition flux, Mar. Pollut. Bull., 206, 116711, https://doi.org/10.1016/j.marpolbul.2024.116711, 2024.
Shelley, R. U., Landing, W. M., Ussher, S. J., Planquette, H., and Sarthou, G.: Regional trends in the fractional solubility of Fe and other metals from North Atlantic aerosols (GEOTRACES cruises GA01 and GA03) following a two-stage leach, Biogeosciences, 15, 2271-2288, https://doi.org/10.5194/bg-15-2271-2018, 2018.
Shelley, R. U., Baker, A. R., Thomas, M., and Murphy, S.: Aerosol trace element solubility and deposition fluxes over the Mediterranean Sea and Black Sea basins, Biogeosciences, 22, 585-600, https://doi.org/10.5194/bg-22-585-2025, 2025.
Shi, J., Guan, Y., Ito, A., Gao, H., Yao, X., Baker, A. R., and Zhang, D.: High Production of Soluble Iron Promoted by Aerosol Acidification in Fog, Geophys. Res. Lett., 47, e2019GL086124, https://doi.org/10.1029/2019GL086124, 2020.
Shi, Z. B., Woodhouse, M. T., Carslaw, K. S., Krom, M. D., Mann, G. W., Baker, A. R., Savov, I., Fones, G. R., Brooks, B., Drake, N., Jickells, T. D., and Benning, L. G.: Minor effect of physical size sorting on iron

760 solubility of transported mineral dust, Atmos. Chem. Phys., 11, 8459-8469, https://doi.org/10.5194/acp-
761 11-8459-2011, 2011.
762 Sholkovitz, E. R., Sedwick, P. N., and Church, T. M.: Influence of anthropogenic combustion emissions on the
763 deposition of soluble aerosol iron to the ocean: Empirical estimates for island sites in the North
764 Atlantic, Geochim. Cosmochim. Acta, 73, 3981-4003, https://doi.org/10.1016/j.gca.2009.04.029, 2009.
765 Song, M., Jeong, R., Kim, D., Qiu, Y., Meng, X., Wu, Z., Zuend, A., Ha, Y., Kim, C., Kim, H., Gaikwad, S.,
766 Jang, K. S., Lee, J. Y., and Ahn, J.: Comparison of Phase States of PM(2.5) over Megacities, Seoul and
767 Beijing, and Their Implications on Particle Size Distribution, Environ. Sci. Technol., 56, 17581-17590,
768 https://doi.org/10.1021/acs.est.2c06377, 2022.
769 Sullivan, R. C., Guazzotti, S. A., Sodeman, D. A., and Prather, K. A.: Direct observations of the atmospheric
770 processing of Asian mineral dust, Atmos. Chem. Phys., 7, 1213-1236, https://doi.org/10.5194/acp-7-
771 1213-2007, 2007.
772 Sun, J., Liu, L., Xu, L., Wang, Y., Wu, Z., Hu, M., Shi, Z., Li, Y., Zhang, X., Chen, J., and Li, W.: Key Role of
773 Nitrate in Phase Transitions of Urban Particles: Implications of Important Reactive Surfaces for
774 Secondary Aerosol Formation, J. Geophys. Res.-Atmos., 123, 1234-1243,
775 https://doi.org/10.1002/2017JD027264, 2018.
776 Takahashi, Y., Higashi, M., Furukawa, T., and Mitsunobu, S.: Change of iron species and iron solubility in Asian
777 dust during the long-range transport from western China to Japan, Atmos. Chem. Phys., 11, 11237-
778 11252, https://doi.org/10.5194/acp-11-11237-2011, 2011.
779 Tang, M., Cziczo, D. J., and Grassian, V. H.: Interactions of Water with Mineral Dust Aerosol: Water
780 Adsorption, Hygroscopicity, Cloud Condensation, and Ice Nucleation, Chem. Rev., 116, 4205-4259,
781 https://doi.org/10.1021/acs.chemrev.5b00529, 2016.
782 Taylor, S. R., and McLennan, S. M.: The continental crust: Its composition and evolution, Blackwell Scientific
783 Publications, Oxford, 312 pp., 1985.
784 Trochkine, D., Iwasaka, Y., Matsuki, A., Yamada, M., Kim, Y.-S., Nagatani, T., Zhang, D., Shi, G.-Y., and Shen,
785 Z.: Mineral aerosol particles collected in Dunhuang, China, and their comparison with chemically
786 modified particles collected over Japan, J. Geophys. Res.-Atmos., 108, 8642,
787 https://doi.org/10.1029/2002JD003268, 2003.
788 Virkkula, A., Teinilä, K., Hillamo, R., Kerminen, V. M., Saarikoski, S., Aurela, M., Viidanoja, J., Paatero, J.,
789 Koponen, I. K., and Kulmala, M.: Chemical composition of boundary layer aerosol over the Atlantic
790 Ocean and at an Antarctic site, Atmos. Chem. Phys., 6, 3407-3421, https://doi.org/10.5194/acp-6-3407-
791 2006, 2006.
792 Walters, W. W., and Hastings, M. G.: Collection of Ammonia for High Time-Resolved Nitrogen Isotopic
793 Characterization Utilizing an Acid-Coated Honeycomb Denuder, Anal. Chem., 90, 8051-8057,
794 https://doi.org/10.1021/acs.analchem.8b01007, 2018.
795 Wang, G. H., Cheng, C. L., Huang, Y., Tao, J., Ren, Y. Q., Wu, F., Meng, J. J., Li, J. J., Cheng, Y. T., Cao, J. J.,
796 Liu, S. X., Zhang, T., Zhang, R., and Chen, Y. B.: Evolution of aerosol chemistry in Xi'an, inland
797 China, during the dust storm period of 2013 - Part 1: Sources, chemical forms and formation
798 mechanisms of nitrate and sulfate, Atmos. Chem. Phys., 14, 11571-11585, https://doi.org/10.5194/acp-
799 14-11571-2014, 2014.
800 Wang, S., Yan, Q., Zhang, R., Jiang, N., Yin, S., and Ye, H.: Size-fractionated particulate elements in an inland
801 city of China: Deposition flux in human respiratory, health risks, source apportionment, and dry
802 deposition, Environmental Pollution, 247, 515-523, https://doi.org/10.1016/j.envpol.2019.01.051,

2019.
Wang, Z., Liu, C., Xie, Z., Hu, Q., Andreae, M. O., Dong, Y., Zhao, C., Liu, T., Zhu, Y., Liu, H., Xing, C., Tan, W., Ji, X., Lin, J., and Liu, J.: Elevated dust layers inhibit dissipation of heavy anthropogenic surface air pollution, Atmos. Chem. Phys., 20, 14917-14932, 10.5194/acp-20-14917-2020, 2020.
Westberry, T. K., Behrenfeld, M. J., Shi, Y. R., Yu, H., Remer, L. A., and Bian, H.: Atmospheric nourishment of global ocean ecosystems, Science, 380, 515-519, https://doi.org/10.1126/science.abq5252, 2023.
Wu, F., Zhang, D., Cao, J., Guo, X., Xia, Y., Zhang, T., Lu, H., and Cheng, Y.: Limited production of sulfate and nitrate on front-associated dust storm particles moving from desert to distant populated areas in northwestern China, Atmos. Chem. Phys., 17, 14473-14484, https://doi.org/10.5194/acp-17-14473-2017, 2017.
Xu, H., and Weber, T.: Ocean Dust Deposition Rates Constrained in a Data-Assimilation Model of the Marine Aluminum Cycle, Global Biogeochem. Cycles, 35, e2021GB007049, https://doi.org/10.1029/2021GB007049, 2021.
Yang, J., Ma, L., He, X., Au, W. C., Miao, Y., Wang, W. X., and Nah, T.: Measurement report: Abundance and fractional solubilities of aerosol metals in urban Hong Kong – insights into factors that control aerosol metal dissolution in an urban site in South China, Atmos. Chem. Phys., 23, 1403-1419, https://doi.org/10.5194/acp-23-1403-2023, 2023.
Zhang, H., Li, R., Dong, S., Wang, F., Zhu, Y., Meng, H., Huang, C., Ren, Y., Wang, X., Hu, X., Li, T., Peng, C., Zhang, G., Xue, L., Wang, X., and Tang, M.: Abundance and Fractional Solubility of Aerosol Iron During Winter at a Coastal City in Northern China: Similarities and Contrasts Between Fine and Coarse Particles, J. Geophys. Res.-Atmos., 127, e2021JD036070, https://doi.org/10.1029/2021JD036070, 2022.
Zhang, H., Li, R., Huang, C., Li, X., Dong, S., Wang, F., Li, T., Chen, Y., Zhang, G., Ren, Y., Chen, Q., Huang, R., Chen, S., Xue, T., Wang, X., and Tang, M.: Seasonal variation of aerosol iron solubility in coarse and fine particles at an inland city in northwestern China, Atmos. Chem. Phys., 23, 3543-3559, https://doi.org/10.5194/acp-23-3543-2023, 2023.
Zhang, L., Kojima, T., and Zhang, D.: Origins and Aging of Calcium-rich Mineral Particles in Asian Dust Arriving in Southwestern Japan: A Comparison of Slow- and Fast-moving Events, Aerosol Sci. Eng., https://doi.org/10.1007/s41810-024-00275-z, 2024.
Zhang, R., Jing, J., Tao, J., Hsu, S. C., Wang, G., Cao, J., Lee, C. S. L., Zhu, L., Chen, Z., Zhao, Y., and Shen, Z.: Chemical characterization and source apportionment of $PM_{2.5}$ in Beijing: seasonal perspective, Atmos. Chem. Phys., 13, 7053-7074, https://doi.org/10.5194/acp-13-7053-2013, 2013.
Zhang, X. Y., Gong, S. L., Shen, Z. X., Mei, F. M., Xi, X. X., Liu, L. C., Zhou, Z. J., Wang, D., Wang, Y. Q., and Cheng, Y.: Characterization of soil dust aerosol in China and its transport and distribution during 2001 ACE-Asia: 1. Network observations, J. Geophys. Res.-Atmos., 108, 4261, https://doi.org/10.1029/2002JD002632, 2003.
Zhi, M., Wang, G., Xu, L., Li, K., Nie, W., Niu, H., Shao, L., Liu, Z., Yi, Z., Wang, Y., Shi, Z., Ito, A., Zhai, S., and Li, W.: How Acid Iron Dissolution in Aged Dust Particles Responds to the Buffering Capacity of Carbonate Minerals during Asian Dust Storms, Environ. Sci. Technol., 59, 6167-6178, https://doi.org/10.1021/acs.est.4c12370, 2025.

Text S1. Sampling sites

At Xi'an, sampling in spring, summer and autumn was conducted on a building roof (~40 m above the ground level) at Shaanxi University of Science and Technology (34°22'N, 108°58'E). This site is surrounded by residential areas, with no major industrial sources nearby. Sampling in winter was carried out on a building roof (~10 m above the ground level) at the Institute of Earth Environment, Chinese Academy of Sciences (34°13'N, 108°53'E). This site is surrounded by commercial and residential areas. Both sampling sites are urban sites (Zhang et al., 2023).

At Qingdao, sampling was conducted on the rooftop of a 5-floor building in northeastern Qingdao (36°20'N, 120°39'E). This rural/suburban site, which is ~28 m above the ground level and ~1.3 km from the coastline, is surrounded by some residence and office buildings, villages and agricultural fields (Zhang et al., 2022).

Table S1. Brief summary of atmospheric sampling at Xi'an and Qingdao.

Location	Season	Sample period	Number of samples
Xi'an	spring	01 to 30 April 2021	28
	summer	12 July to 14 August 2021	32
	autumn	07 October to 06 November	30
	winter	01 November to 30 December 2020	36
Qingdao	spring	20 March to 22 April 2023	28
	summer	20 June to 26 July 2022	26
	autumn	04 to 31 October 2022	27
	winter	23 November to 24 December 2022	25

Table S2. Summary of total aerosol Al concentrations (μg/m^3) measured over East Asian and the Pacific Ocean.

Location	Geographic coordinates	Sampling period	Size range	Average	Range	reference
Aksu, China	40°16'N, 80°28'E	May to June 2001	TSP	24	/	Zhang et al. (2003)
Urumqi, China	43°49'N, 87°37'E	January 2004 to March 2007	TSP	8.05	/	Li et al. (2008)
Wuhai, China	39°39'N, 106°49'E	March 2021	$PM_{2.5}$	7.77±19.15	0.00-195.79	Meng et al. (2023)
Xi'an, China	34°22'N, 108°58'E	November 2020 to November 2021	d_p > 1 μm	1.42±0.86	0.16-3.70	This study
			d_p < 1 μm	2.28±2.35	0.14-14.88	
Yulin, China	38°17'N, 109°28'E	Spring 2006-2008	TSP	36.38 (dust)	/	Wang et al. (2011)
				6.91 (non-dust)	/	
Beijing, China	39°97' N, 116°21'E	March to May 2012	$PM_{2.5}$	3.97±1.26 (dust)	/	Liu and Bei (2016)
				0.76±0.61 (non-dust)	/	
Jinan, China	36°40'N, 117°09'E	March 2021	$PM_{2.5}$	1.10±2.56	0.00-20.68	Meng et al. (2023)
Qingdao, China	36°20'N, 120°39'E	November 2022 to March 2023	d_p > 1 μm	0.56±0.75	0.08-4.01	This study
			d_p < 1 μm	1.08±1.67	0.05-9.63	
Huaniao Island, China	30°51'N, 122°40′E	April 2010 to March 2011	TSP	/	0.075-16	Guo et al. (2014)
Higashi-Hiroshima, Japan	34°24'N, 132°42'E	December 2012 to December 2013	TSP	/	0.17-1.716	Sakata et al. (2023)
The Pacific Ocean (Hawaii)	21°15′N, 157°45′W	January and June 2002	TSP	/	0.001-0.056	Measures et al. (2010)
The Pacific Ocean	along 30°N	June to August 2004	TSP	0.078	0.012-0.475	Buck et al. (2013)

Table S3. Overview of total aerosol Al concentrations (μg/m^3) for submicron and supermicron particles at Xi'an and Qingdao.

Location	Season	submicron particles			supermicron particles		
		range	mean	median	range	mean	median
Xi'an	spring	0.14-14.88	4.29±3.70	3.32	0.25-3.70	1.54±0.89	1.59
	summer	0.17-2.01	0.95±0.44	0.90	0.16-1.96	0.96±0.54	0.97
	autumn	0.20-2.26	1.06±0.48	1.03	0.22-2.75	1.22±0.72	1.07
	winter	0.32-6.11	2.92±1.47	3.02	0.31-3.53	1.91±0.93	1.91
Qingdao	spring	0.18-9.63	1.88±2.51	0.93	0.29-3.69	1.04±1.12	0.48
	summer	0.05-0.85	0.35±0.22	0.35	0.08-0.63	0.33±0.18	0.37
	autumn	0.27-1.32	0.65±0.22	0.63	0.13-0.57	0.31±0.12	0.30
	winter	0.40-9.17	1.40±1.82	0.81	0.12-4.01	0.51±0.77	0.29

Table S4. Overview of dissolved aerosol Al concentrations (ng/m^3) for submicron and supermicron particles at Xi'an and Qingdao.

Location	Season	submicron particles			supermicron particles		
		range	mean	median	range	mean	median
Xi'an	spring	0.3-359.4	65.4±79.2	40.1	1.2-47.2	23.1±10.9	24.8
	summer	3.3-100.9	23.2±23.4	17.3	3.6-37.2	15.0±8.7	13.1
	autumn	6.0-120.2	22.6±20.1	19.3	1.2-37.0	13.2±8.6	12.5
	winter	3.1-97.3	25.6±19.8	22.1	9.2-43.7	19.6±8.2	17.5
Qingdao	spring	2.5-20.9	8.7±5.8	6.2	1.1-41.3	8.8±10.8	5.3
	summer	0.4-30.6	10.2±8.2	8.9	1.3-40.2	12.8±11.1	9.4
	autumn	1.3-23.0	6.0±4.8	5.2	0.3-49.0	7.9±10.5	3.5
	winter	1.8-63.3	14.5±15.2	9.4	1.4-54.9	12.8±12.9	8.9

Table S5. Overview of aerosol Al solubility (%) for submicron and supermicron particles at Xi'an and Qingdao.

Location	Season	submicron particles			supermicron particles		
		range	mean	median	range	mean	median
Xi'an	spring	0.11-7.74	1.46±1.48	1.01	0.45-4.84	1.75±1.04	1.38
	summer	0.74-9.10	2.40±2.03	1.69	0.76-4.71	1.83±0.95	1.59
	autumn	1.21-7.36	2.23±1.40	1.82	0.25-2.64	1.17±0.54	1.04
	winter	0.31-3.55	0.99±0.75	0.74	0.43-7.70	1.42±1.47	1.01
Qingdao	spring	0.14-4.23	0.93±1.02	0.61	0.06-8.91	1.58±2.29	0.54
	summer	0.11-11.11	3.27±2.55	2.33	0.69-12.79	4.55±3.61	3.56
	autumn	0.18-3.44	1.01±0.86	0.69	0.18-14.77	2.74±3.56	1.17
	winter	0.32-5.03	1.26±1.05	0.93	0.30-23.35	4.21±5.35	2.39

Table S6. Overview of total Al (μg/m^3), dissolved Al (ng/m^3) and Al solubility (%) under different weather conditions for submicron and supermicron particles at Xi'an.

	submicron particles			supermicron particles		
total Al	range	average	median	range	average	median
entire	0.14-14.88	2.28±2.35	1.40	0.16-3.70	1.42±0.86	1.31
clean	0.28-6.73	1.67±1.39	1.30	0.16-2.49	1.07±0.58	1.13
dust	2.75-14.88	8.54±4.24	8.40	0.92-3.70	2.25±1.06	2.22
haze	0.32-5.94	2.59±1.32	2.21	0.31-3.53	2.08±0.91	2.23
dissolved Al	range	average	median	range	average	median
entire	0.3-359.4	33.1±44. 7	20.4	1.15-47.3	17.7±9.7	16.3
clean	0.3-125.8	28.1±25.3	21. 7	1.21-37.2	14.6±8.3	13.4
dust	54.1-359.4	146.1±109.6	139.1	24.8-47.2	34.5±8.7	34.3
haze	7.6-80.8	20.0±21.1	15.0	11.3-43.7	22.2±9.3	21.2
Al solubility	range	average	median	range	average	median
entire	0.11-9.10	1.75±1.57	1.32	0.25-7.70	1.54±1.10	1.22
clean	0.11-9.10	1.96±1.62	1.64	0.25-4.71	1.51±0.75	1.29
dust	0.42-7.74	2.31±2.49	1.86	0.77-4.84	2.08±1.55	1.47
haze	0.31-3.22	0.96±0.71	0.72	0.43-7.70	1.49±1.71	1.01

Table S7. Overview of total Al (μg/m^3), dissolved Al (ng/m^3) and Al solubility (%) under different weather conditions for submicron and supermicron particles at Qingdao.

	submicron particles			supermicron particles		
total Al	range	average	median	range	average	median
entire	0.05-9.63	1.08±1.67	0.68	0.08-4.01	0.56±0.75	0.36
clean	0.08-1.34	0.66±0.28	0.68	0.08-1.15	0.31±0.17	0.30
dust	1.05-9.63	6.42±3.08	7.14	0.66-4.01	2.90±1.10	2.96
haze	0.77-1.90	1.40±0.58	1.55	0.47-1.09	0.69±0.35	0.50
fog	0.18-1.09	0.53±0.35	0.42	0.17-0.52	0.38±0.14	0.37
dissolved Al	range	average	median	range	average	median
entire	0.4-63.3	9.8±9.6	6.1	0.3-54.9	10.5±11.4	6.3
clean	0.4-40.6	6.2±5.7	5.4	0.9-26.6	5.1±5.0	3.0
dust	2.5-63.3	25. 9±20.9	20.6	1.9-23.6	11.5±7.5	10.4
haze	24.5-26.6	25.4±1.1	25.2	14.2-39.7	23.7±14.0	17.3
fog	4.0-19.5	7.4±5.5	5.2	8.7-54.6	29.4±17.2	34.8
Al solubility	range	average	median	range	average	median
entire	0.11-11.11	1.60±1.78	0.91	0.06-23.35	3.23±3.95	1.70
clean	0.11-8.30	1.15±1.26	0.77	0.18-15.58	2.10±2.72	0.99
dust	0.20-1.50	0.45±0.47	0.24	0.06-2.87	0.67±0.98	0.31
haze	1.40-3.27	2.09±1.03	1.58	2.85-3.70	3.40±0.47	3.64
fog	0.43-4.23	1.93 ±1.52	1.38	2.37-23.35	9.09±7.26	6.90

Table S8. Pearson correlations coefficient (*r*): aerosol Al solubility versus [sulfate]/[Al] and [nitrate]/[Al] for submicron and supermicron particles at Xi'an and Qingdao. In this table, *r* values which are >0.5 are highlighted in bold.

Species	Season	Xi'an		Qingdao	
		submicron particles	supermicron particles	submicron particles	supermicron particles
[sulfate]/[Al]	spring	-0.33	0.33	**0.87**	**0.75**
	summer	-0.17	0.36	**0.68**	**0.66**
	autumn	0.15	**0.58**	**0.59**	**0.84**
	winter	**0.57**	**0.73** (0.41*)	0.17	**0.96**
[nitrate]/[Al]	spring	-0.37	0.25	**0.89**	**0.71**
	summer	-0.20	0.29	0.14	**0.59**
	autumn	-0.12	**0.70**	**0.70**	**0.90**
	winter	0.32	**0.93** (0.44*)	0.30	**0.88**

* Pearson correlations coefficients (r) after three outliers for which aerosol Al solubility was very high were excluded.

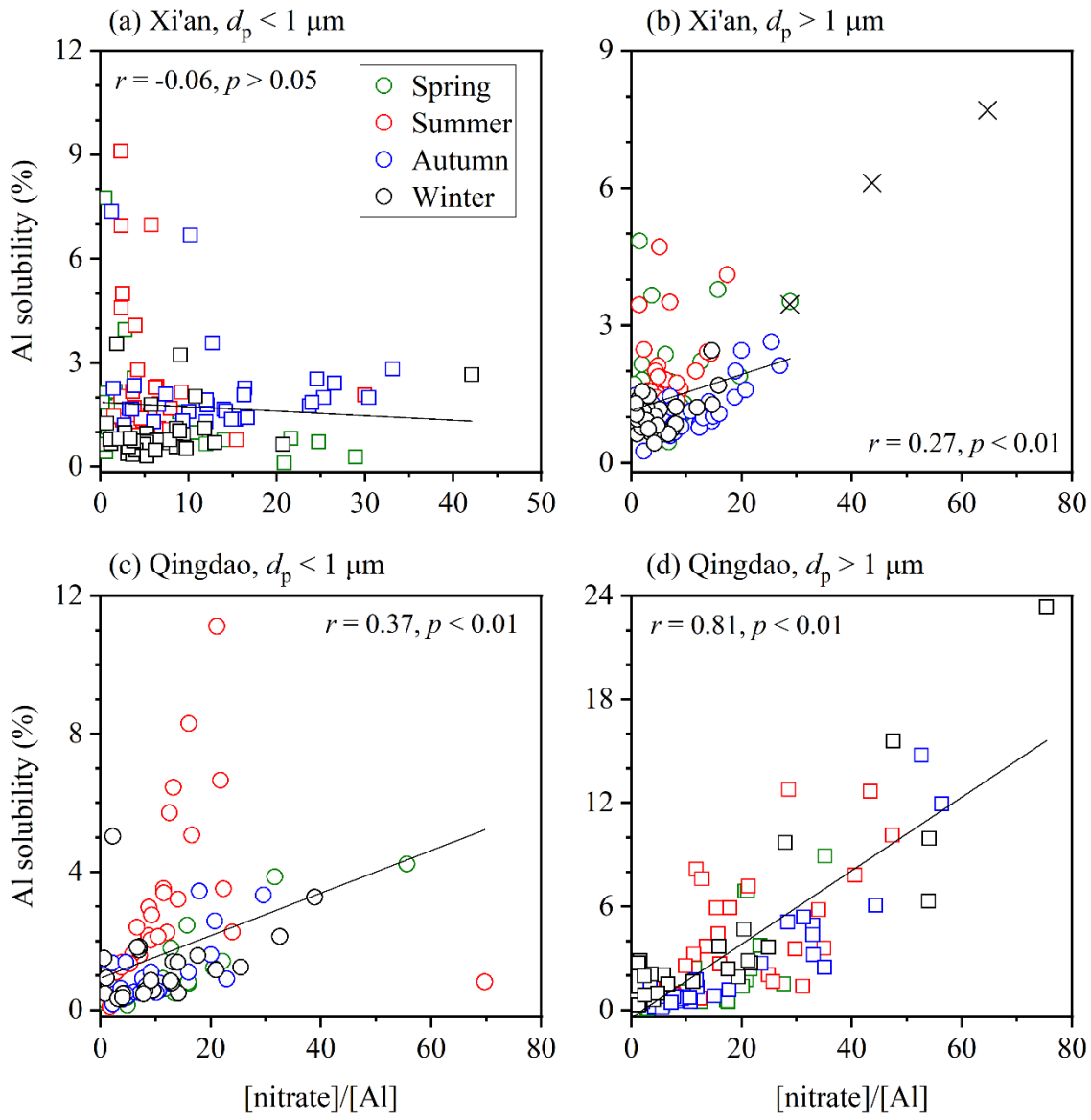

Figure S1. Aerosol Al solubility versus [nitrate]/[Al]: (a) submicron particles at Xi'an; (b) supermicron particles at Xi'an; (c) submicron particles at Qingdao; (d) supermicron particles at Qingdao (the *r* value changed from 0.81 to 0.77 if the data point with the highest Al solubility was excluded). Data represented by crosses are not included in fittings.

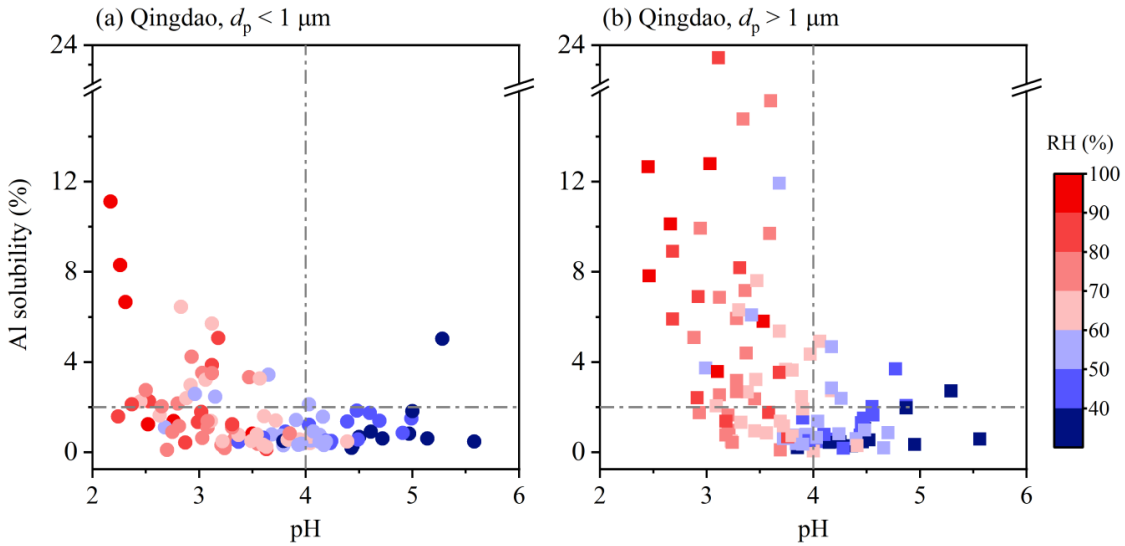

Figure S2. Dependence of aerosol Al solubility on relative humidity (RH) and aerosol pH at Qingdao: (a) submicron particles; (b) supermicron particles.

References

Buck, C. S., Landing, W. M., and Resing, J.: Pacific Ocean aerosols: Deposition and solubility of iron, aluminum, and other trace elements, Mar. Chem., 157, 117-130, https://doi.org/10.1016/j.marchem.2013.09.005, 2013.

Guo, L., Chen, Y., Wang, F., Meng, X., Xu, Z., and Zhuang, G.: Effects of Asian dust on the atmospheric input of trace elements to the East China Sea, Mar. Chem., 163, 19-27, https://doi.org/10.1016/j.marchem.2014.04.003, 2014.

Li, J., Zhuang, G., Huang, K., Lin, Y., Xu, C., and Yu, S.: Characteristics and sources of air-borne particulate in Urumqi, China, the upstream area of Asia dust, Atmos. Environ., 42, 776-787, https://doi.org/10.1016/j.atmosenv.2007.09.062, 2008.

Liu, Q., and Bei, Y.: Impacts of crystal metal on secondary aliphatic amine aerosol formation during dust storm episodes in Beijing, Atmos. Environ., 128, 227-234, https://doi.org/10.1016/j.atmosenv.2016.01.013, 2016.

Measures, C. I., Sato, T., Vink, S., Howell, S., and Li, Y. H.: The fractional solubility of aluminium from mineral aerosols collected in Hawaii and implications for atmospheric deposition of biogeochemically important trace elements, Mar. Chem., 120, 144-153, https://doi.org/10.1016/j.marchem.2009.01.014, 2010.

Meng, Q., Yan, C., Li, R., Zhang, T., Zheng, M., Liu, Y., Zhang, M., Wang, G., Du, Y., Shang, C., and Fu, P.: Variations of PM2.5-bound elements and their associated effects during long-distance transport of dust storms: Insights from multi-sites observations, Sci. Total Environ., 889, 164062, https://doi.org/10.1016/j.scitotenv.2023.164062, 2023.

Sakata, K., Sakaguchi, A., Yamakawa, Y., Miyamoto, C., Kurisu, M., and Takahashi, Y.: Measurement report: Stoichiometry of dissolved iron and aluminum as an indicator of the factors controlling the fractional solubility of aerosol iron – results of the annual observations of size-fractionated aerosol particles in Japan, Atmos. Chem. Phys., 23, 9815-9836, https://doi.org/10.5194/acp-23-9815-2023, 2023.

Wang, Q., Zhuang, G., Li, J., Huang, K., Zhang, R., Jiang, Y., Lin, Y., and Fu, J. S.: Mixing of dust with pollution on the transport path of Asian dust — Revealed from the aerosol over Yulin, the north edge of Loess Plateau, Sci. Total Environ., 409, 573-581, https://doi.org/10.1016/j.scitotenv.2010.10.032, 2011.

Zhang, H., Li, R., Dong, S., Wang, F., Zhu, Y., Meng, H., Huang, C., Ren, Y., Wang, X., Hu, X., Li, T., Peng, C., Zhang, G., Xue, L., Wang, X., and Tang, M.: Abundance and Fractional Solubility of Aerosol Iron During Winter at a Coastal City in Northern China: Similarities and Contrasts Between Fine and Coarse Particles, J. Geophys. Res.-Atmos., 127, e2021JD036070, https://doi.org/10.1029/2021JD036070, 2022.

Zhang, H., Li, R., Huang, C., Li, X., Dong, S., Wang, F., Li, T., Chen, Y., Zhang, G., Ren, Y., Chen, Q., Huang, R., Chen, S., Xue, T., Wang, X., and Tang, M.: Seasonal variation of aerosol iron solubility in coarse and fine particles at an inland city in northwestern China, Atmos. Chem. Phys., 23, 3543-3559, https://doi.org/10.5194/acp-23-3543-2023, 2023.

Zhang, X. Y., Gong, S. L., Shen, Z. X., Mei, F. M., Xi, X. X., Liu, L. C., Zhou, Z. J., Wang, D., Wang, Y. Q., and Cheng, Y.: Characterization of soil dust aerosol in China and its transport and distribution during 2001 ACE-Asia: 1. Network observations, J. Geophys.

Res.-Atmos., 108, 4261, https://doi.org/10.1029/2002JD002632, 2003.